Student thesis series INES nr 547

Topographic controls of drought impact on Swedish primary forests

Johanna Asch

2021
Department of
Physical Geography and Ecosystem Science
Lund University
Sölvegatan 12
S-223 62 Lund
Sweden

Johanna Asch (2021).
Topographic controls of drought impact on Swedish primary forests

Master degree thesis, 30 credits in *Physical Geography and Ecosystem Analysis*
Department of Physical Geography and Ecosystem Science, Lund University

Level: Master of Science (MSc)

Course duration: *January* 2021 until *June* 2021

Disclaimer

Topographic controls of drought impact on Swedish primary forests

---

Johanna Asch

Master thesis, 30 credits, in *Physical Geography and Ecosystem Science*

Supervisor
Anders Ahlström
Dep. of Physical Geography and Ecosystem Science, Lund University

Exam committee:
Stefan Olin, Dep. of Physical Geography and Ecosystem Science, Lund University

Tristan Bakx, Dep. of Physical Geography and Ecosystem Science, Lund University

Acknowledgements

This thesis would not have been possible without the great supervision of Anders Ahlström. Thank you Anders, for guiding me through this project, and also for your enthusiasm and love for science that helped keep up my motivation while working from home. My sincerest thanks to Julika Wolf for her help and expertise, and for always being available to answer my questions. Without her excellent work in her own thesis, and her help with Google Earth Engine, this thesis would not have happened. I would also like to express my gratitude to Katarina Georgiou for her advice regarding modelling with random forests.

Moreover, I would like to thank Gudrun Jensdóttir, Maximilian Huber and Max Mangold for the exceptional food, and for the friendship that kept me sane during these weird times. Thanks to my family and to Nic Tarasewicz for their very helpful feedback and for always having a kind, open ear. Lastly, I would like to thank Ross Folkard for his unconditional, loving support and healthy rational perspective.

Abstract

Anthropogenic climate change has increased the frequency of extreme drought events and leads to “hotter” droughts. Boreal forests will experience the largest temperature increase among global forests and may be particularly at risk. Topography controls plant available water and site-specific climatic conditions. Drought sensitivity may therefore vary over short distances between wet and dry locations of the landscape. However, topography is rarely included as a factor in research investigating vegetation dynamics. Due to being located in often complex terrain and growing in unmanaged conditions, primary forests offer the opportunity to study the influence of topography on the impact of droughts on vegetation in natural ecosystems. This study investigated the role of the local environment and topography in controlling drought impact of the 2018 summer drought in primary forests in Sweden, by applying a random forest modelling approach. Drought effects were modelled using summer 2018 Landsat EVI2 anomalies (z-scores) as a function of predictor variables including terrain indices, bioclimatic variables, and forest properties. Topographic predictors included primary terrain indices such as aspect, slope, and the Topographic Position Index (TPI) as well as the more complex compound terrain indices the Topographical Wetness Index (TWI) and Hight Above Nearest Drainage (HAND). The most influential variables were selected with a recursive feature elimination approach, creating a model with 13 predictors.

The final model explained 48% (R^2 = 0.48) of the variance in an independent subset of EVI2 anomalies. Primary terrain indices described the spatial variability of z-scores better than compound terrain indices. Forest located on steep slopes, high topographic positions, and south facing aspects were associated with negative z-scores, indicative of reduced primary productivity. Valley bottoms and north-facing aspects mostly showed no or positive drought impact. Drought effects, meaning EVI2 anomalies were more negative with increasing distance to wetlands. These topographic and wetland effects on drought impact were seen across all forest types and latitudes, however the severity of negative drought impact differed between forest classes and was more pronounced in the south. The results clearly show that the impact of the 2018 summer drought was strongly controlled by the local terrain in Swedish primary forests, highlighting the importance of incorporating topography in studies aimed at quantifying and predicting drought impact on vegetation. Previous research suggests that primary forests were less affected by the 2018 drought than managed forests were. This analysis suggests that the widespread drainage of wetlands and establishment of monocultures in managed forests may explain this difference. Forest management may therefore exacerbate the future impact of potentially more severe and more frequent droughts.

Keywords: Physical geography, ecosystem analysis, primary forest, boreal forest, drought impact, topography, drainage, climate change, random forest, terrain index

Table of Contents

List of abbreviations

CART	Classification And Regression Tree
CIT	Conditional Inference Tree
DEM	Digital Elevation Model
DNW	Distance to Nearest Wetland
DTW	Depth To Water
EVI	Enhanced Vegetation Index
EVI2	Two-band Enhanced Vegetation Index
GPP	Gross Primary Production
HAND	Hight Above Nearest Drainage
MSE	Mean Square Error
NDVI	Normalized Difference Vegetation Index
NIR	Near-infrared Reflectance (0.7-1.2μm)
OOB	Out-Of-Bag
R	Red Reflectance (0.6-0.7μm)
RMSE	Root Mean Square Error
RF	Random Forest
RFE	Recursive Feature Elimination
scPDSI	Self-calibrating Palmer Drought Severity Index
SM	Soil Moisture Index
STI	Soil Topographic Wetness Index
TPI	Topographic Position Index
TWI	Topographic Wetness Index
%Inc MSE	Percent increase of the mean square error

1. Introduction

Anthropogenic climate change has led to increases in frequency and intensity of extreme weather events such as droughts in the last decades (IPCC 2014). These changes, especially moisture stress due to recent drought events, have had negative effects on the health and productivity of forest ecosystems worldwide (Allen et al. 2010; Senf et al. 2018). Due to being located in the high latitudes, boreal forest ecosystems are projected to be particularly strongly affected by future changes in climate conditions, experiencing the largest temperature increase among global forest systems (Gauthier et al. 2015; Seidl et al. 2017). The most recent extreme drought event was the drought affecting central Europe and Scandinavia in summer 2018, which resulted in substantial decreases of carbon uptake in many ecosystems (Bastos et al. 2020; Lindroth et al. 2021). However, the impact of drought events can vary quite significantly between and within forest ecosystems in the same climate zone (Cartwright et al. 2020; Schwartz et al. 2020; Lindroth et al. 2021). This spatial heterogeneity is caused by many factors including topography, species distribution, and soil composition (Fekedulegn et al. 2003; Kharuk et al. 2020; Schwartz et al. 2020). Therefore, to predict forest ecosystem responses to future drought events accurately, it is crucial to study the site specific drought impact in detail (Hawthorne and Miniat 2018; Schwartz et al. 2019).

One challenge in remote sensing studies of ecosystems is the unknown influence of human management. In forests, this includes the harvesting of trees, which may be difficult to separate from natural disturbances. One way to avoid such complications is to study unmanaged, primary ecosystems where no management or harvest occurs. Swedish primary forests are usually situated in topographically heterogenous regions with higher altitude and steeper slopes than secondary forests, making them ideal study sites for increasing our understanding of how topography and water access modify drought effects (Ahlström et al. 2020). Topography as an important local modulator of drought response has been studied mainly in tropical and temperate forest ecosystems (Fekedulegn et al. 2003; Pasho et al. 2012; Schwartz et al. 2019; Schwartz et al. 2020). It can either aggravate moisture stress or mitigate negative drought effects (Pasho et al. 2012; Cartwright et al. 2020). These effects are usually studied using simple terrain indices such as slope, aspect, and elevation. Trees on steep and south facing slopes are generally associated with increased negative drought impact, whereas trees growing on north facing slopes and in valley bottoms are less negatively affected (Huang and Anderegg 2012; Schwartz et al. 2019; Cartwright et al. 2020; Kharuk et al. 2020). Aspect and slope influence water availability and the amount of received solar radiation and, therefore, the local drought severity (Huang and Anderegg 2012; Schwartz et al. 2019). More complex, compound terrain indices, such as the topographic wetness index (TWI) and hight above nearest drainage (HAND) offer more precise predictions of soil moisture and landform by combining primary indices and could therefore be better suited to investigate drought effects (Nobre et al. 2011; Ågren et al. 2014; Buchanan et al. 2014; Muukkonen et al. 2015). Additionally, since primary forest in Sweden

were not subject to draining, distance to the nearest wetlands could have an influence on the moisture status of forests and therefore modulate drought effects.

However, the influence of topography on drought impact is not well characterised. To our knowledge no study has investigated the relationship between different topographical indices and drought impact on boreal primary forests in detail. The aim of this thesis is, therefore, to analyse if topography was an important modifier of the 2018 drought in primary forests in Sweden, as well as identifying the most suitable terrain indices for describing these drought effects through answering the following research questions.

1. Was topography a significant regulator of drought impact on primary forests in Sweden in 2018?

2. Which terrain index or combination of indices is most suited for describing spatial patterns of drought impact on primary forests in Sweden?

2. Background

2.1 "Hotter droughts" and their effect on the land carbon sink

Droughts and their effects are studied from many different disciplinary perspectives; therefore, no universal definition of the term exists (Wilhite and Glantz 1985). For the purpose of this study, the focus will be on the meteorological and agricultural definitions of droughts. Meteorological droughts are predominantly described as periods of time with a precipitation deficit greater than a certain threshold in relation to a long-term average ("normal") (Wilhite and Glantz 1985; Mishra and Singh 2010). Agricultural droughts link the meteorological drought to the impact on agriculture, usually in combination with an increasing soil moisture deficit (Wilhite and Glantz 1985; Mishra and Singh 2010). Anthropogenic climate change has been shown to aggravate drought events, leading to "hotter droughts" also called "global-change-type droughts" (Breshears et al. 2005; Allen et al. 2015). These droughts are characterized by heatwaves coinciding with precipitation deficits (Allen et al. 2015; Buras et al. 2020). Rising temperatures also exacerbate soil moisture depletion by increasing atmospheric demand for water, leading to an increase in occurrence of soil moisture droughts (Hanel et al. 2018).

With Europe experiencing a decreasing trend of soil moisture levels over the last 40 years and temperatures projected to rise with climate change, co-occurrence of precipitation deficits and heat waves can be expected to increase significantly in the future (Copernicus Climate Change Service 2018; Samaniego et al. 2018; Hari et al. 2020). Europe has already experienced a number of these extreme drought events in the last 30 years, some of the most recent and extreme being the droughts affecting large parts of the continent during the summer heat waves in 2003 and 2018 (Mishra and Singh 2010; Buras et al. 2020). The 2018 drought was

particularly severe in its duration and extent and differed from 2003 with its location over central and northern Europe as opposed to southern Europe (Bastos et al. 2020; Buras et al. 2020). According to the European state of the climate report for 2018, summer 2018 was the hottest summer on record with soil moisture levels reaching a record low. In some areas of central and northern Europe precipitation was less than 80 % of the seasonal average for spring, summer and autumn (Copernicus Climate Change Service 2018). These droughts had a significant effect on the land carbon sink, resulting in decreased vegetation productivity and significant yield losses (Bastos et al. 2020).

In 2003 and 2018, the summer droughts were preceded by unusually warm springs (Bastos et al. 2020). Even though spring warming could partially balance out the decreased vegetation productivity in summer through an earlier onset and accelerated growth in spring, it also aggravated the summer soil moisture deficits. Soil moisture resources were depleted faster by the additional biomass increasing water-stress on the vegetation in summer (Bastos et al. 2020). Gross primary productivity (GPP) decreased an estimated 30 % in 2003, reversing the previous four years of net carbon sequestration (Ciais et al. 2005). Thompson et al. (2020) found positive annual net ecosystem exchange anomalies (compared to the 10-year mean) in northern Europe in 2018. This carbon loss was caused by a reduced carbon uptake in summer 2018. Summer GPP decreased by 38% in grasslands and 10 % in forests during the 2018 drought (Fu et al. 2020).

Due to its location over central and northern Europe the 2018 drought presents an ideal opportunity for studying the effects of hotter droughts on forests in Sweden. Summer 2018 was the hottest summer on record in some parts of Sweden such as Götaland and Svealand. July was one of the warmest on record and accompanied by a prolonged drought for most of Sweden. On average it was a drier than normal summer with areas receiving less than half of the normal precipitation. However, drought effects across Sweden were heterogeneous, some areas of northern Sweden such as northern Norrland received a precipitation surplus (SMHI 2018).

2.2 Drought and forest health

Drought conditions influence the relative rates of water uptake and loss in plants, changing the internal water balance and inducing water stress. High temperatures and atmospheric vapor pressure deficits increase the vapor pressure from leaf to air, inducing water loss through evapotranspiration (Kramer 1963). Plants respond to water deficits by closing their stomata. However, this reduces the diffusion of air and, therefore, carbon dioxide into the plant, which slows down photosynthesis. Additionally, water-stress directly affects photosynthesis since dehydrated cells have a decreased capacity for photosynthesis (Kramer 1963). If photosynthesis rates decrease until the plants metabolism cannot be maintained, the plant is at risk of carbon starvation (Allen et al. 2010). Low soil moisture conditions impair the plants' capacity for compensating the increased transpiration though water uptake from the soil. If drought

conditions persist this can result in hydraulic failure through cavitation in the xylem (water-transporting tissue) (McDowell et al. 2008). Cavitation refers to the process of local vaporisation of the transported liquid filling the xylem with water vapor. The plant can therefore no longer move water, leading to tissue damage and eventually death (McDowell et al. 2008; Allen et al. 2010). Additionally, water stress weakens tree defences against pathogens and insect attacks (Allen et al. 2010).

Rising temperature and increased frequency of drought events due to anthropogenic climate change have already had a noticeable impact on forest health worldwide (Allen et al. 2015; Gauthier et al. 2015; Seidl et al. 2017; Senf et al. 2018). Goulden and Bales (2019) reported a significant increase in tree mortality, as a consequence of the 2012-2015 extended drought period in California. In Europe, the area of canopy mortality in temperate forests has doubled over the period of 1984 to 2016, a trend observed across different forest types and countries (Senf et al. 2018). In boreal forests of North America background forest mortality rates have increased substantially in recent decades (Allen et al. 2010).

Boreal forests play an essential role in global temperature regulation and carbon budgets (Bonan 2008; Gauthier et al. 2015). They comprise around 30 % of the global forest cover and are estimated to contribute around 20 % of the global carbon sink (Pan et al. 2011; Gauthier et al. 2015). Because of their locations in high latitudes, boreal forests have been experiencing particularly high increases in climate change related disturbances, triggered by warming temperatures and drought induced water stress (IPCC 2014; Seidl et al. 2017). As a consequence, a reduction of the carbon sink has been observed in forests in northwest Canada, where biomass accumulation rates decreased since 2003. With prolonged climate change these forests could turn from a net carbon sink to a carbon source (Ma et al. 2012). Boreal forests in Siberia have experienced an increased mortality of Siberian pine and fir, caused by moisture stress, elevated temperatures, and increased insect attacks (Kharuk et al. 2020). Despite increased pressure on boreal forests the number of studies investigating drought effects in detail is still low, especially for the European boreal regions.

2.3 Primary forests

Primary forests are commonly defined as “naturally regenerated forest of native species, where there are no clearly visible indications of human activities and the ecological processes are not significantly disturbed” (FAO 2010). Additionally, primary forests can be defined by stand age, forest area, and the time since past human disturbance (Buchwald 2005). The terminology for primary forest in literature is inconsistent, primary forests are often interchangeably referred to as “old-growth” or “pristine” forests. Here, the term primary forests will be used referring to the definition by the FAO (2010) and the terminology presented by Buchwald (2005).

It has been hypothesised that primary forests are carbon neutral due to reduced growth rates and increased respiration of mature trees. Recently, this assumption has been challenged by research showing that primary forests are significant carbon sinks (Luyssaert et al. 2008). In Europe, most of the primary forests are found in the boreal zone, with the largest area estimated to be located in Sweden (Sabatini et al. 2018; Ahlström et al. 2020). However, Swedish primary forests have only recently been catalogued and described by Ahlström et al. (2020) and very little research about them exists. Primary forests occur predominantly in remote areas of complex terrain in high altitudes and latitudes (Sabatini et al. 2018; Ahlström et al. 2020). With climate change disproportionately affecting boreal and mountainous forest ecosystems, primary forests and their carbon storage potential are highly threatened by increased temperatures and droughts (Allen et al. 2010; Gauthier et al. 2015; Seidl et al. 2017). In contrast to the majority of Swedish boreal forests, primary forests have been spared from intensive management. Most forests in Sweden are monocultures of Norway spruce or Scots pine and were subjected to extensive draining in the past (Hånell 1988; Jönsson et al. 2015; Jacks 2019). In primary forests however, natural composition of native species and forested wetlands are still intact. Wetlands, for example, could influence the spatial heterogeneity of drought effects, by mitigating drought effects on nearby forests. Research investigating the influence of wetlands on drought impact on forests is sparce. Primary forests, therefore, provide the opportunity to study forest responses to climate change under unmanaged conditions, which could additionally provide insights on the impact of forest management, such as draining, on drought resistance.

2.4 Local variations in forest drought response

Drought impact can vary spatially on a global or continental scale but also on a local scale. Topography determines the hydrological patterns of the environment and plays an important part in creating local “microclimates” or “topoclimates”, which are characterized by regional climatic influences and local terrain (Dobrowski 2011; Adams et al. 2014). The climate that organisms experience at a certain location, therefore, varies spatially with topographic position (Thornthwaite 1953; Dobrowski 2011). Consequently, drought sensitivity of the vegetation is variable across space since drought effects are mitigated or aggravated by complex local interactions (Dobrowski 2011; Pasho et al. 2012; Adams et al. 2014; Cartwright et al. 2020; Schwartz et al. 2020). Generally, vegetation is topographically organised, biomass tends to decrease with increasing elevation and vegetation productivity is elevated at convergent topographic positions (e.g. valleys) compared to divergent positions (e.g. ridges) (Swetnam et al. 2017; Hoylman et al. 2019). This organisation has been observed to be particularly pronounced in areas experiencing climatic water limitations (Hoylman et al. 2019). Drought can, therefore, be expected to amplify differences between topographic positions, leading to spatial variations of carbon uptake and forest growth with implications for the local carbon budget (Adams et al. 2014). With climate warming and more frequent drought stress, especially in mountainous and high latitude forests, it becomes increasingly important to understand the

interactions of climate, local terrain, and vegetation (Dobrowski 2011; Swetnam et al. 2017; Hoylman et al. 2019). At drier topographic positions (divergent), such as high elevations, steep slopes, and southern facing aspects, drought and increased temperatures could significantly increase water-stress (Schwartz et al. 2019; Schwartz et al. 2020).

Sites of high elevation relative to their surroundings are usually more exposed and have low water retention potentials. They are therefore more closely linked to the atmospheric environment, meaning they are more directly influenced by climate variations than more protected areas e.g. in valley bottoms (Dobrowski 2011; Hawthorne and Miniat 2018; Cartwright et al. 2020). Several studies have observed a more severe drought impact on vegetation growing on higher elevations (Muukkonen et al. 2015; Hawthorne and Miniat 2018; Cartwright et al. 2020). However, depending on the structure and climatic location of the environment, the direction and intensity of topographic influences can vary significantly (Dobrowski 2011). Local temperature at points with the same elevation can vary greatly depending on their topographic position in the landscape (Dobrowski 2011). In complex topographical regions elevation is, therefore, likely to be only a weak predictor of local drought effects (Dobrowski 2011; Huang and Anderegg 2012). Additionally, in some regions, due to increased precipitation and lower temperatures in high mountainous regions, negative drought impact could decrease at high altitudes (Kharuk et al. 2020). In these regions slope and slope aspect may have greater influences on the local microclimate (Letts et al. 2009; Kimball et al. 2017; Park et al. 2019).

Slope mainly influences local water retention and runoff, but also the amount of received solar radiation and soil composition (Pasho et al. 2012). Drought effects have been shown to increase in severity with increasing slope (Pasho et al. 2012; Schwartz et al. 2019; Kharuk et al. 2020). However, the effect is suspected to be greater in arid regions or xeric sites and less pronounced in temperature limited regions (Fridley 2009; Dobrowski 2011). Received solar radiation differs drastically between slope aspects. Soil moisture is, therefore, generally greater at north-facing locations than on south-facing slopes (Miller and Poole 1983). When soil moisture limits plant growth, high solar radiation and increased evaporation on south-facing aspects can increase the severity of negative drought effects (Letts et al. 2009). This was seen in many forest ecosystems across different climate zones. In tropical forests and North American temperate forests negative drought impact and tree mortality were increased on south and west facing slopes (Huang and Anderegg 2012; Anderegg et al. 2015; Goulden and Bales 2019; Schwartz et al. 2019). This could also be observed in some boreal forest ecosystems, however, studies investigating the interaction between topography and drought in boreal forest ecosystems are rare. Kharuk et al. (2020) found a link between drought induced mortality of Siberian pine and fir and topography. Mortality increased with increasing steepness and on south facing slopes (Kharuk et al. 2020). During drought events in Canada, southern aspects showed increased leaf temperature and leaf-to-air vapour pressure and decreased stomatal conductance (Letts et al.

2009). Muukkunen et al. (2015) found drought impact to be more severe on hill summits than lower lands in boreal forests in Finland.

Influences of slope and slope aspect on plant stress are complex and highly species dependent (Fekedulegn et al. 2003; Letts et al. 2009). Species compositions changes along the slope and species growing in different topographical positions have different water use strategies (Kimball et al. 2017). Consequently, species-specific stomatal regulation in interaction with topography plays an important role in the vegetation response to drought (Kimball et al. 2017; Hawthorne and Miniat 2018). Because of their adaptation to low soil moisture environments species growing on mesic sites may be better adapted to cope with drought (Kimball et al. 2017).

Their characteristics (section 2.3) suggest that primary forests in Sweden could be strongly controlled by their topographic environment. This is why, this study aims at investigating if topographic organisation of vegetation drought response described in literature can be found in these forests.

2.5 Terrain indices derived from digital elevation models

Hydrological, atmospheric, and ecological processes are strongly influenced by characteristics of the land surface. Modelling landforms and their influence on hydrology, vegetation, and climate is therefore crucial for studying these processes (Wilson 2012). Digital elevation models (DEM) usually provide the base for analysis of the land surface. Many parameters can be derived from DEMs and used to describe the terrain. In contrast to complex hydrological modelling approaches, deriving these land surface parameters or "terrain indices" needs less computational power and is less time consuming. They can easily be applied over large areas at relatively high resolutions (Wilson 2012; Buchanan et al. 2014). However, the performance of terrain indices is heavily dependent on the quality and resolution of the underlying DEM (Wilson 2012).

2.5.1 Primary terrain indices

Primary terrain indices or land surface parameters can be derived directly from the DEM without additional information (Wilson 2012). Local primary terrain indices such as slope and aspect focus on relationships between neighbouring raster cells or data points. Regional primary terrain indices take larger areas into account, for example flow path length and upslope contributing area (in the following also referred to as "flow accumulation") (Wilson 2012). Both examples are based on flow direction estimations derived from the DEM (Wilson 2012). A variety of algorithms exist for the calculation of flow direction. Single flow routing algorithms such as the algorithm *D8,* consider only one cell when estimating the down slope flow direction. Multiple flow routing algorithms such as the algorithm $D\infty$, consider two or more cells in the flow direction estimation (Wilson 2012; Ågren et al. 2014; Buchanan et al.

2014). The best performing algorithm depends on the application (e.g. soil moisture estimation, vegetation mapping) and the resolution of the DEM (Kopecký and Čížková 2010; Ågren et al. 2014; Buchanan et al. 2014).

2.5.2 Compound terrain indices

Up-slope contributing area in combination with slope is used in many secondary terrain indices (Ågren et al. 2014). Secondary or "compound" terrain indices usually combine primary terrain indices or require additional input data. They can be divided into hydrological surface parameters and solar radiation models (Wilson 2012). Secondary terrain indices usually provide a better estimate of hydrological patterns in the landscape (Buchanan et al. 2014). The topographical wetness index (TWI) is one of the most widely used compound terrain indices (Wilson 2012; Buchanan et al. 2014). It was developed by Beven and Kirby (1979) and describes the relative moisture status of a location as a function of local slope and up-slope contributing area. The index has been applied in many studies and has been shown to model soil moisture moderately well (Schmidt and Persson 2003; Kopecký and Čížková 2010; Ågren et al. 2014; Buchanan et al. 2014; Raduła et al. 2018). For example, in a random forest approach to predict areas experiencing severe drought. Park et al. (2019) found the TWI to be an important parameter, but less important than slope and aspect. TWI has also been applied in landscape ecology studies. It has been shown to be an important factor in forest succession and was spatially correlated with basal area increment growth rates and forest biomass (Swetnam et al. 2017; Vidal-Macua et al. 2017; Hoylman et al. 2018). In a study investigating drought impact on boreal forests in Finland, Muukkunen et al. (2015) identified TWI as an important indicator in predicting the positions of risk areas in the landscape.

A relatively new compound terrain index, height above nearest drainage (HAND), was developed by Rennó et al. (2008). HAND is a proxy for a locations drainage potential by calculating the vertical distance between the location and the nearest point of drainage (Rennó et al. 2008; Nobre et al. 2011). It was developed to model local environments in relation to soil water conditions in Amazonian forests. Since then, it has been used in several studies to model vegetation distribution and composition in relation to water table depth in tropical forests (Schietti et al. 2014; Esteban et al. 2021). Additionally, HAND has been applied in hydrological studies including flood prediction and river channel geometry modelling where it produced results comparable to complex hydrological models (Afshari et al. 2018; Zheng et al. 2018; Johnson et al. 2019).

A widely applied index for describing the relative position of a point in the landscape is the topographic position index (TPI). TPI is a measure of the elevation of the cell relative to the mean elevation of the surrounding cells in a specific neighbourhood (Weiss 2001; Ågren et al. 2014). It provides a measure of moisture status on a hillslope scale and has been applied in vegetation ecology studies investigating local vegetation productivity, biomass, and climate sensitivity (Swetnam et al. 2017; Hoylman et al. 2018; Hoylman et al. 2019). Swetnam et al.

(2017), for example, found topographic position an important factor in the distribution of carbon storage in forest catchments in Colorado (United States). It can additionally be used in combination with slope for landform classifications to identify ridges, hillslopes, and valleys (Weiss 2001). Kramm et al. (2017) compared the TPI classification approach to other approaches, and found it performed with high accuracies, comparable to more complex approaches such as object-based image analysis. However, according to De Reu et al. (2013), TPI failed to model real terrain structures for strongly heterogenous landscapes. In these landscapes, deviation from mean elevation, which describes topographic position based on TPI and the standard deviation of the elevation, may constitute a better suited index (De Reu et al. 2013).

2.6 Vegetation indices

Remote sensing provides an opportunity to study large scale vegetation changes over time and space. Vegetation indices are commonly used to enhance the vegetation signal in the remotely sensed data. They take advantage of the spectral properties of vegetation in the red (R) and the near-infrared (NIR) spectral region by combining satellites bands of these wavelengths (Chuvieco 2016). Photosynthetically active vegetation absorbs light in the R spectrum and strongly reflects NIR wavelengths. The most commonly applied vegetation index is the normalized difference vegetation index (NDVI) (Chuvieco 2016). However, NDVI saturates in high biomass regions and is thus not well suited for densely forested areas (Huete et al. 2002). The enhanced vegetation index (EVI) and its 2 - band EVI derivative (EVI2) show improved sensitivity to high biomass canopies (equation 1) (Huete et al. 2002; Jiang et al. 2008). EVI and EVI2 are strongly correlated to GPP and can be used as a direct estimation of GPP in different forests ecosystems (Rahman et al. 2005; Sims et al. 2006; Schubert et al. 2012). Therefore, they have been applied in studies investigating changes in forest primary productivity under drought conditions (Reinermann et al. 2019; Schwartz et al. 2019; Buras et al. 2020).

2.7 Random forest algorithm

Random forest (RF) is a powerful machine learning algorithm developed by Breiman (2001), based on the aggregation of many decision trees ("classification and regression trees" - CART), used in classification and regression problems. Each tree is built with a random subset of the training data, this process is also called bootstrap aggregating or "bagging". For each tree therefore a part of the training data is excluded from the building process the so called "out-of-bag" (OOB) data. This reduces variance, increases the stability of the algorithm and can be used to assess model performance, by computing the mean square error (MSE) of each tree with the OOB data (Breiman 2001; Grömping 2009). The tree is built from the root node with the first splitting of "branches". Each split is based on a specified number of predictor variables randomly selected from all variables (mtry). Because of the randomness introduced by these properties each tree will be built slightly differently. The overall prediction of the RF is the

average prediction of all trees (Breiman 2001). In natural sciences, random forests have been increasingly applied in recent years for example for selection and classification of genes and for landcover classifications (Díaz-Uriarte and Alvarez de Andrés 2006; Zhang and Yang 2020). It allows for the analysis of large complex data sets with high numbers of variables and non-linear relationships between variables. Additionally, its structure provides relatively high interpretability compared to other machine learning approaches and it can provide a measure of variable importance (Grömping 2009; Zhang and Yang 2020). Recently, random forest regressions have also been applied in studies investigating predictors of drought impact. Schwartz et al. (2019) investigated the influence of forest properties and topography on drought effects in tropical forests with a RF regression approach. Park et al. (2019) used topographic and remote sensing data for the prediction of areas affected by severe drought in Korea based on random forest. For this study, RF provides the opportunity to perform a unified regression analysis of potential drought impact predictors and identify the most influential predictors, covering both research questions.

3. Materials and methods

3.1 Primary forest map

Primary forests used in this project were extracted from a digital map containing polygons of primary forests in Sweden (unpublished). This map was created and updated based on a primary forest inventory 1978 - 1981 by the Swedish environmental protection agency and the Swedish forest agency and is described in more detail in Ahlström et al. (2020). The map also contained information on past human disturbance, protection type, status, duration, as well as a ranking of pristineness based on the framework established by Buchwald (2005). For this analysis, areas disturbed by forest fires in 2018 and forests ranked with a pristineness level below 5 were excluded. As shown in figure 1, the remaining 348 polygons are distributed over the whole of Sweden with the largest stretches of primary forests situated in the north western part of the country along the border to Norway. The approach was first tested with one primary forest (Skuleskogen forest) and then extended to include all primary forests.

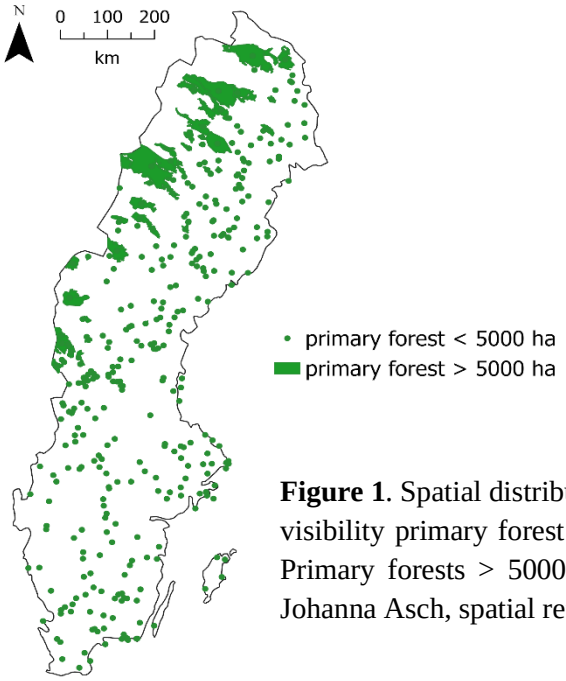

Figure 1. Spatial distribution of primary forests in Sweden. For increased visibility primary forest with areas < 5000 ha are represented as points. Primary forests > 5000 ha are presented as polygons (green). Author: Johanna Asch, spatial reference system: SWEREF99 TM.

3.2 EVI2 z-scores

For quantifying drought effects on the vegetation, EVI2 was calculated for July and September 2018 and compared to the 2008- 2017 baseline period. Data retrieval and EVI2 calculation were done in Google Earth Engine by adapting a script provided by Julika Wolf and following methods described by Wolf (2020). Landsat 5, 7 and 8 surface reflectance satellite data (TM/ETM+/OLI sensors) were extracted, and clouds and cloud shadows were masked out using the quality assessment bands ("pixel_qa" bands). EVI2 values were calculated according to equation 1 with band 3 (R) and 4 (NIR) of Landsat 5 and 7 data and band 4 (R) and 5 (NIR) of Landsat 8 data.

$$EVI2 = 2.5 * \frac{\rho_{NIR} - \rho_R}{\rho_{NIR} + 2.4 * \rho_R + 1}$$

Equation 1, where ρ_R refers to satellite bands in the red and ρ_{NIR} refers to satellite bands of the near-infrared region of the wave spectrum.

For additional cloud filtering, EVI2 values smaller than 0.15 were excluded. July – September median EVI2 composites were created for the summer of 2018 and the baseline years. EVI2 scores were normalized against the baseline by calculating z-scores. Z-scores were derived by subtracting the mean of the baseline EVI2 composites from the 2018 July – September composite and dividing it by the standard deviation of the baseline (equation 2) (Wolf 2020).

$$z - score = \frac{EVI2_{2018} - EVI2_{baseline}}{EVI2_{baseline\ SD}}$$

Equation 2, where $EVI2_{2018}$ and $EVI2_{baseline}$ stand for the July – September mean EVI2 for 2018 and the baseline years (2008 – 2017). $EVI2_{baseline\ SD}$ refers to the standard deviation of the baseline EVI2.

The EVI2 rasters were further processed with ArcGIS pro 2.6.0 (© 2020 Esri Inc.), where they were projected to SWEREF99 TM, and resampled to 50m cell size with bilinear interpolation (resolution of the DEM used). The z-scores were analysed against terrain indices and other environmental variables.

3.3 DEM derived terrain indices

All terrain indices were calculated in ArcGIS pro based on a DEM of Sweden with 50 m spatial resolution, retrieved from Lantmäteriet (Lantmäteriet 2021). An overview of all indices is shown in table 1.

3.3.1 Primary terrain indices

Slope was calculated in degrees with the planar method, using the average maximum technique. Aspect was computed using the default planar method in ArcGIS pro, which determines the compass direction in degrees from 0 - 360 (north - north) of the downhill slope using a 3x3 cell moving window. The aspect was transformed with cos(aspect[in radian]), so aspect values range from -1.0 (south) to 1.0 (north), and 0 representing east and west.

3.3.2 TPI

TPI was calculated according to Weiss (2001), using the ArcGIS tool "Topographic Position Index (Jenness)" from the toolbox "Topography Tools 10_2_1" developed by Dilts (2015) based on ArcView 3.3 tools by Jenness (2006) (equation 3 and 4).

$$TPI = z_0 - \bar{z}$$

$$\bar{z} = \frac{1}{n_r} \sum_{i \epsilon r} z_i$$

Equation 3 and 4, where z_0 is the elevation of the central cell and $\bar{z}$ is the mean elevation of the neighbourhood with the radius r.

Negative TPI values indicate lower landscape positions such as valleys and lower slopes. High topographic positions such as upper slopes and ridges have positive TPI values. The range of

the unitless values depends on the study site and the neighbourhood used in the calculation. The index is sensitive to the scale of the neighbourhood and optimal neighbourhood size differs according to the study area and the purpose of the analysis. Therefore, it was calculated with different circular neighbourhood radii of 1000 m, 500 m, and 250 m, respectively (De Reu et al. 2013). Large neighbourhoods provide topographic positions in relation to larger scale areas, while small neighbourhoods allow to differentiate small depressions and local hills. Analysis of Skuleskogen TPI data against EVI2 data showed the best fit for a neighbourhood with 1000 m radius. This is why, neighbourhood sizes of 1000 m and 4000 m were chosen for the Sweden wide analysis.

3.3.3 TWI

TWI was derived by creating flow direction and flow accumulation rasters using the D8 algorithm (Buchanan et al. 2014). The D8 algorithm was chosen based on findings by Buchanan et al. (2014) showing that single flow direction algorithms perform better for coarse DEMs than more complex algorithms incorporating multiple flow directions. TWI was calculated using the slope and flow accumulation rasters according to equation 5 and smoothed with a 3x3 low-pass filter (Beven and Kirkby 1979; Buchanan et al. 2014). Due to a lack of sufficiently high-resolution data, the TWI calculation was not modified to include soil transmissivity.

$$TWI = \ln\left(\frac{\alpha}{\tan\beta}\right)$$

Equation 5, where α refers to flow accumulation and β to slope in radian.

3.3.4 HAND

HAND of each cell was derived following HAND model procedure first described by Rennó et al. (2008). For this a stream raster was created from the flow accumulation raster using a threshold of 400 cells. The stream raster was converted into points and used together with the flow direction to create watersheds. The watersheds were processed with zonal statistics to determine the minimum elevation of each watershed. The HAND model was calculated by subtracting the minimum elevation of the watersheds from the DEM.

3.4 Other environmental variables

3.4.1 Soil moisture map

To compare the solely topography derived terrain indices to a more complex soil moisture estimation, a national soil moisture index (SM) map made available by the Swedish Environmental Protection Agency was used (Naturvårdsverket 2019a). The SM combines depth to water (DTW) with a modified version of the TWI, the Soil Topographic Wetness Index (STI) with a weighting of 70 % DTW and 30 % STI. The STI includes the soil transmissivity (speed of horizontal movement of water through the soil), which is based on soil type information from

the geological survey of Sweden (SGU) (Naturvårdsverket 2021). STI has been shown to produce more accurate soil moisture estimates on a regional scale (Buchanan et al. 2014). However, due to a lack of soil data for mountain ranges only the TWI was calculated for these regions.

3.4.2 Distance to nearest wetland (DNW)

A national land cover map "Nationella Marktäckedata 2018", was retrieved from the Swedish Environmental Protection Agency (Naturvårdsverket 2019b). The map was reclassified to only include wetlands. Distance to the nearest wetland (DNW) was derived by calculating the Euclidian distance of each cell to the nearest cell classified as wetland in the land cover map. The rasters were resampled from their original 10 m resolution to the 50 m resolution of the DEM.

3.4.3 Forest classes

The national land cover map "Nationella Marktäckedata 2018", was additionally used for information on forest types and to exclude non forested areas (Naturvårdsverket 2019b). The map was reclassified to only include the 14 forest types (classes 111-117 and 121-127, excluding temporarily non-forested areas in classes 118 and 128), which were then further reclassified to the broad forest categories: 1 = pine forest, 2 = spruce forest, 3 = coniferous mixed forest, 4 = deciduous coniferous forest, 5 = deciduous forest. The rasters were resampled with bilinear interpolation from their original 10 m resolution to the 50 m resolution of the DEM.

3.4.4 scPDSI

The self-calibrating Palmer Drought Severity Index (scPDSI) was retrieved (0.5° by 0.5° resolution), projected to SWEREF99 TM and mean values were calculated per pixel for July – September (Barichivich et al. 2018). The scPDSI is a drought index based on precipitation and temperature observational data from the CRU TS v4.03 climate dataset and includes a simple water balance model, as well as parameters adapted to the characteristics of the local climate (Wells et al. 2004; van der Schrier et al. 2013).

3.4.5 Bioclimatic variables

Bioclimatic variables at 30 arc s resolution (~ 1km) were retrieved from the "WorldClim" Database (Fick and Hijmans 2017). The rasters were projected to SWEREF99 TM. Bioclimatic variables describe annual and seasonal climate conditions influencing organisms' physiology (Noce et al. 2020). In this analysis bioclimatic variables were included to account for the influence of different climatic conditions over Sweden on forest drought response. The WorldClim dataset is widely used and provides 19 bioclimatic variables for the period 1970 – 2000 (Fick and Hijmans 2017; Noce et al. 2020). A list of bioclimatic variables used in the analysis is presented in table 1.

3.4.6 Stand age and canopy height

Stand age and canopy height rasters of 25 m resolution provided by SLU (Swedish University of Agricultural Science) (SLU 2010). The rasters were resampled to 50 m resolution.

3.5 Statistical analysis

For the statistical analysis random samples were taken from the data by extracting cell values at 165 000 randomly selected points from all data layers described in section 3.3 and 3.4 in ArcGIS pro. All subsequent analysis was done in R Studio (RStudio Team 2020). After excluding No Data points, 164 473 points were used for all primary forests for further analysis. The number of sample points possible to include for subsequent analysis with a random forest regression was restricted by available computational power.

3.5.1 Random forest regression

A first random forest model (RF 1) of EVI2 z-scores was trained with all 33 explanatory variables described in section 3.3 and 3.4 (in the following also referred to as predictors) to determine the most important factors driving the spatial variability of drought impact. An overview of all included variables is shown in table 1. The model was built using the R package randomForest (Liaw and Wiener 2002). The randomForest package is based on the random forest algorithm RF-CART first developed by Breiman (2001). The sample data was split randomly into a training (75%) and validation (25%) dataset. Random forests provide an assessment of the model performance in capturing the training data by calculating the out-of-bag mean square error (OOB-MSE). As described in section 2.7, for each tree in the model, due to random sampling roughly one third of observations are "out of the bag" (OOB), and not used in the tree. Tree predictive performance can, therefore, be assessed by calculating the MSE of tree prediction and OOB data. The model error is then calculated with the OOB-MSE from each tree. Additionally, the algorithm estimates the "pseudo" R^2 (1 – OOB-MSE / Variance(z-scores)), a measure for how much of the variance of the training data is captured by the forest. Both metrics were used to assess model performance during the model tuning and variable selection process. For the purpose of higher interpretability, the model OOB-MSE was transformed to OOB-RMSE (root mean square error), since the units of the RMSE are equivalent to z-scores. A random forest with 500 trees, splitting 4 variables (mtry = 4) at each node was used for all runs. The number of trees was kept at the default setting (500 trees) after assessing the OOB-MSE for trees from 1-500. Breiman (2001) suggested an mtry of n predictors/3 for regression approaches. However, according to Grömping (2009) RF-CART models are relatively insensitive to variations in mtry. To save computational time the influence of reducing the number of variables per split (mtry) was analysed using the tuneRF function, estimating the OOB-MSE for each mtry. Decreasing mtry to 4 did not change the OOB-MSE significantly and was therefore set for all following runs.

Selection of important predictors was done using the permutation variable importance measure included in the R package, where importance is determined by the percentage increase of the model MSE, if the variable was permuted (%Inc MSE). To assess the impact of a given variable on the model the OOB-MSE of the tree is calculated. Then the predictor is permuted, meaning in this case it is randomly shuffled to introduce noise, and the OOB prediction error is recorded again. The difference between both errors, averaged over all trees and normalized by the standard deviation is defined as the permutation variable importance (Grömping 2009). For predictors with no influence on the model, the difference between both errors should be close to zero.

Variable selection was performed with a modified recursive feature elimination (RFE) approach. In RFE predictors are reduced one by one, repeating that process several times and assessing model R^2 and MSE for each iteration (Pullanagari et al. 2018). Here, a modified version of the approach was applied, due to limitation in computational power. Features were eliminated by assessing variable importance of the first model (RF 1) and excluding predictors with variable importance below 10 %Inc MSE. This process was repeated with a %Inc MSE threshold of 20% until the model R^2 started to decrease notably with further variable elimination. It resulted in a final model (RF4) with 13 explanatory variables with %Inc MSE > 20%.

Partial dependence plots were produced from the final model. Partial dependence plots describe the partial relationship between EVI2 z-scores and each variable when the other variables are set to their average values. They allow visualization of the model's response to individual explanatory variables and assessment of model performance in capturing known trends. The distribution of data points was indicated in each partial dependence plot using deciles. Additionally, two variable partial dependencies were produced using the R package pdp (Greenwell 2017). For two variable partial dependencies, all but two variables of interest were set to their average value and partial relationships were calculated with RF4.

A model validation was performed with the test data set by using the model to predict z-scores with the predictor data set in the test data and comparing them to the observed EVI2 z-scores of the test data. To assess model performance R^2 and RMSE were calculated.

Table 1. List of indices included in the analysis.

Index	Description
Elevation	Elevation above sea level (m)
Slope	In degree (planar, average maximum)
Aspect	Northness, ranges from -1 (S) to 1 (N)
Topographic position index (TPI) (1000m and 4000 m neighbourhood)	Position of each cell relative to the elevation of its specified neighbourhood (equation 3 and 4).
Topographic wetness index (TWI)	Relative moisture status of a cell (equation 5).
Hight above nearest drainage (HAND)	Vertical distance between a cell and the nearest stream (m).
Soil moisture index (SM)	Combination of depth to water (DTW) and Soil Topographic Wetness Index (STI) (Naturvårdsverket 2019a).
Self-calibrating Palmer Drought Severity Index (scPDSI)	Drought index based on observational data, a simple water balance model and regional parameters (Barichivich et al. 2018)
Forest class	Broad forest classes determined by dominant tree type, based on land cover data from Naturvårdsverket (2019b)
Canopy height	Canopy height in m (SLU 2010)
Stand age	Stand age in years (SLU 2010)
Distance to nearest wetland (DNW)	Euclidian distance to nearest cell in wetland based on land cover data from Naturvårdsverket (2019b)
	All following Bio variables: WorldClim data base (Fick and Hijmans 2017)
Bio1	Annual mean temperature (°C)
Bio2	Mean diurnal range (mean of monthly max - min T) (°C)
Bio3	Isothermality (Bio2/Bio7 x 100) (%)
Bio4	Temperature seasonality (sd x 100) (°C)
Bio5	Max temperature of warmest month (°C)
Bio6	Min temperature of warmest month (°C)
Bio7	Temperature annual range (Bio5-6) (°C)
Bio8	Mean temperature of wettest quarter (°C)
Bio9	Mean temperature of driest quarter (°C)
Bio10	Mean temperature of warmest quarter (°C)
Bio11	Mean temperature of coldest quarter (°C)
Bio12	Annual precipitation (mm)
Bio13	Precipitation of wettest month (mm)
Bio14	Precipitation of driest month (mm)
Bio15	Precipitation seasonality (coefficient of variation) (%)
Bio16	Precipitation of wettest quarter (mm)
Bio17	Precipitation of driest quarter (mm)
Bio18	Precipitation of warmest quarter (mm)
Bio19	Precipitation of coldest quarter (mm)

4. Results

4.1 Feature selection

The models created in the process of RFE with variables ranked by their permutation variable importance are presented in table 2 and 3. Excluding variables lead to a significant change in the ranking of variables in the following model. However, certain variables such as DNW, bio18, bio16, Aspect, Slope, Forest class and scPDSI were ranked as top predictors in most models (table 2 and 3). Other variables such as TPI (1000m) increased in variable importance when excluding explanatory variables using RFE or showed considerable changes between models such as latitude (table 2). The bioclimatic variable bio18 (precipitation of warmest quarter), followed by bio16 (precipitation of wettest quarter) and scPDSI showed the strongest impact on the OOB-MSE in the final model (table 3). Of the terrain indices, slope, aspect and TPI (1000m) (ranked in that order) were included in RF4 as important predictors of drought impact on primary forests (table 3). All topographic variables in RF4 were primary terrain indices (slope, aspect, TPI), no compound terrain index (HAND, TWI) was placed in the final model. Of the variables describing forest properties the predominant tree species, represented by the variable “forest class” ranked highest (table 3).

Table 2. Variables and their respective permutation variable importance of intermediate random forest models RF1, RF2 and RF3, created in the recursive feature elimination process. Variable importance is expressed in percent increase of the model OOB-MSE (%IncMSE) when the variable is permuted. A detailed description of the variables can be found in table 1. Dotted lines represent the %IncMSE thresholds set for feature elimination.

RF 1		**RF 2**		**RF 3**	
Variable	%IncMSE	Variable	%IncMSE	Variable	%IncMSE
Aspect	96.85	bio18	62.49	scPDSI	49.35
bio2	61.78	DNW	61.04	Forest class	48.72
DNW	55.82	Latitude	59.83	Stand age	44.15
bio3	52.90	Slope	43.02	bio16	40.84
scPDSI	49.85	scPDSI	41.25	bio9	37.54
bio16	47.55	Stand age	38.87	Canopy height	37.14
Forest class	42.18	bio16	38.13	DNW	33.67
bio7	40.95	Forest class	37.27	Slope	31.47
Elevation	38.54	bio4	37.01	Aspect	30.96
bio18	37.24	Aspect	31.30	TPI (1000 m)	30.83
bio9	32.90	bio3	31.10	bio4	30.29
bio4	32.77	bio2	31.04	Latitude	26.45
Canopy height	31.26	Canopy height	30.78	bio18	21.98
bio10	31.15	bio7	28.75	Elevation	19.26
bio11	23.80	bio6	28.60	bio7	16.81
bio8	21.72	TPI (1000 m)	26.94	TPI (4000 m)	13.39
bio6	19.28	Elevation	23.50	bio3	10.85
TPI (1000 m)	19.03	TPI (4000 m)	23.43	bio2	10.44
bio1	19.01	bio9	20.45	bio6	6.76
HAND	18.32	bio10	12.33		
Latitude	17.02	SM	11.27		
TPI (4000 m)	17.00	HAND	8.93		
Stand age	15.98	bio11	8.62		
Slope	15.80	bio8	7.20		
SM	15.52	bio1	5.36		
TWI	9.58				
bio15	7.68				
bio19	7.44				
bio5	6.11				
bio17	4.43				
bio14	2.33				
bio13	2.21				
bio12	1.56				

Table 3. Variables and their respective permutation variable importance of the final random forest model RF4, created in the recursive feature elimination process. Variable importance is expressed in percent increase of the model OOB-MSE (%IncMSE) when the variable is permuted. A detailed description of the variables can be found in table 1.

RF 4	
Variable	%IncMSE
bio18	75.49
bio16	59.35
scPDSI	59.05
bio9	57.29
Forest class	54.90
bio4	52.28
Slope	42.69
Canopy height	42.45
Aspect	35.46
Latitude	31.23
Stand age	30.86
DNW	28.67
TPI (1000 m)	28.25

As shown in table 4, 20 predictors could be excluded from RF1 to RF4 without increasing the OOB-RMSE substantially. The prediction error of RF4 for the OOB-data (OOB-RMSE) was increased by 0.016 z-scores compared to RF 1, built with all variables (table 4). The final model was comprised of 13 variables with an OOB-RMSE of 0.548 z-scores and an OOB-R^2 of 0.448. The OOB-R^2- value is a measure of the fraction of the variance in the OOB-data captured by the decision trees. Both, the OOB-R^2 and the OOB-RMSE were relatively stable over the first 3 models and decreased more strongly for the final model RF4 (table 4). This stronger reduction of the model error was seen as an indicator that model performance would decrease significantly with further variable reduction. Therefore, the remaining variables were included in the final model.

Table 4. Number of predictors, out-of-bag prediction error in z-scores (OOB-RMSE) and out-of-bag R^2 (OOB-R^2) of the random forest models RF1, RF2, RF3 and RF4, created during the recursive feature elimination process.

	RF 1	**RF 2**	**RF 3**	**RF 4**
Nr. variables	33	25	19	13
OOB-R^2	0.485	0.479	0.473	0.448
OOB-RMSE	0.532	0.535	0.538	0.548

4.2 Model validation

Model validation of RF2 and RF4 z-score prediction performance with a new, independent set of randomly selected locations (41100 grid cells) is presented in figure 2. RF4 predicted z-scores with an RMSE of 0.52 z-scores and an R^2 of 0.48 compared to observed EVI2 z-scores (figure 2). In comparison to the model's capacity to predict the training data z-scores (OOB-RMSE = 0.548), the model performed, therefore, equally well with a new predictor dataset (figure 2B and table 4).

Compared to model RF2, which predicted z-scores with an R^2 of 0.51 and an RMSE of 0.50, RF4 performed similarly well, justifying the reduction of the predictor variables to the final 13. However, the model failed to capture the whole distribution of the test data. Model z-score predictions ranged from approximately -2 to 2, failing to capture the tails of the distribution, i.e. strong negative and positive Z-score anomalies (-5 to 3) (figure 2B).

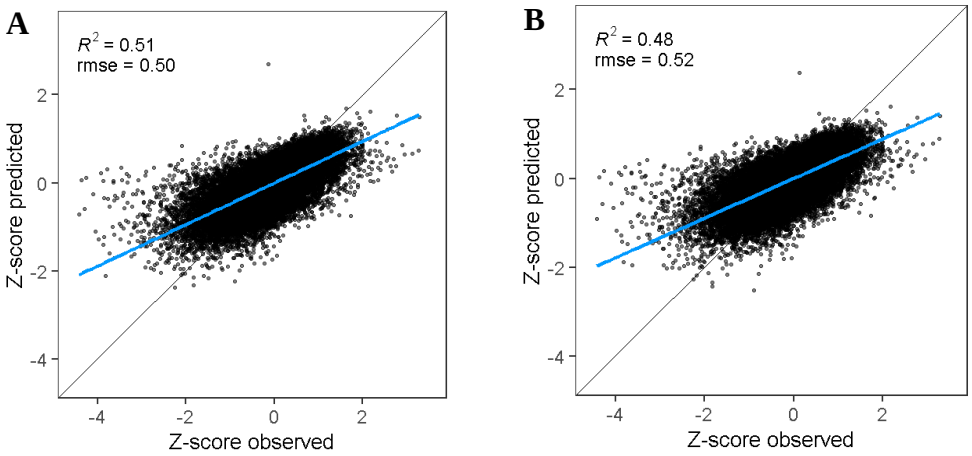

Figure 2. Validation of random forest model RF2 (A) and RF4 (B). Z-scores predicted by the models are plotted against observed July-September 2018 Landsat EVI2 z-scores. RMSE in z-scores, R^2-values and regression lines (blue) were calculated for each model. Validation was performed with independent test data (41100 data points), representing 50 x 50 m grid cells. RF2 prediction was based on 22 predictors and RF4 prediction was based on 13 predictors. A detailed overview of model predictors can be found in table 2 and 3.

4.3 Partial dependencies

For comparison, the spatial distributions of z-scores, scPDSI and bioclimatic variables are presented as maps (figure 3). Partial relationships between each predictor of RF4 and z-scores are shown in figure 4. Comparing the spatial distribution of z-scores with these variables, allows for an assessment of model performance in capturing spatial patterns. In general, model partial dependencies of scPDSI and bioclimatic variables agreed with the spatial patterns presented in the maps. Regions with less precipitation in the wettest (bio16) and warmest (bio18) quarter as well as high temperature seasonality (bio4) showed lower z-scores, i.e. negative drought impact (figure 4). Bio9, the mean temperature of the driest quarter did not show a clear relationship to z-scores. Regions with bio 9 < -10 °C showed higher z-scores than regions with bio9 > -10 and < -5. Additionally, regions with bio 9 > -5 °C, for example in the north west and south west showed increased z-scores as well, explaining the sinusoidal nature of the partial dependence plot (figure 3 and 4). As shown in figure 3, negative z-score anomalies were stronger in the south of Sweden and decreased with increasing latitude. This pattern was captured by the RF4 model as indicated by the positive relationship of latitude and z-scores in the partial dependence plot (figure 4).

The drought index scPDSI shows strong relation to vegetation drought response. Regions with negative scPDSI scores representing regions estimated to have experienced a negative drought impact in summer 2018, were linked to negative z-scores in RF4. Regions with positive scPDSI scores were associated with positive z-scores. However, this was not true for scPDSI > 1.5. ScPDSI scores come at a significantly coarser resolution than EVI2 z-scores and therefore capture only average drought effects (figure 3). Regions in northern central Sweden, experiencing negative z-scores during summer 2018, were thus not captured by the drought index, leading to a mismatch between both variables for scPDSI > 1.5.

Sites receiving more solar radiation such as south facing aspects and high topographic positions were associated with negative z-scores and, thus, were more negatively impacted by the 2018 summer drought. In contrast, forest areas receiving less radiation and potentially storing more water such as north facing aspects and valleys showed positive EVI2 anomalies, indicating increased productivity. Additionally, and also likely linked to water availability, forests located on wetlands (DNW = 0) showed no deviation of EVI2 scores from the baseline (z-scores = 0) and negative z-score anomalies increased with increasing distance to wetland. Partial dependencies to slope showed z-scores increasing with increasing slope until approximately 10° and decreasing for slopes above 10° (figure 4).

Drought effects differed notably between forests classes. Pine dominated locations (forest class 1) were the most impacted forests, showing strong negative z-score anomalies (z-scores < -0.1). Spruce forests showed no negative impact overall (z-scores = 0) (forest class 2), and mixed coniferous forests were situated in between (z-scores > 0.1) (forest class 3). Broadleaved and mixed with coniferous species forests were generally associated with positive z-scores (figure 4). Canopy height and stand age showed no clear trend in their partial relationship, affecting only a small range of z-scores between 0 and -0.05 (figure 4).

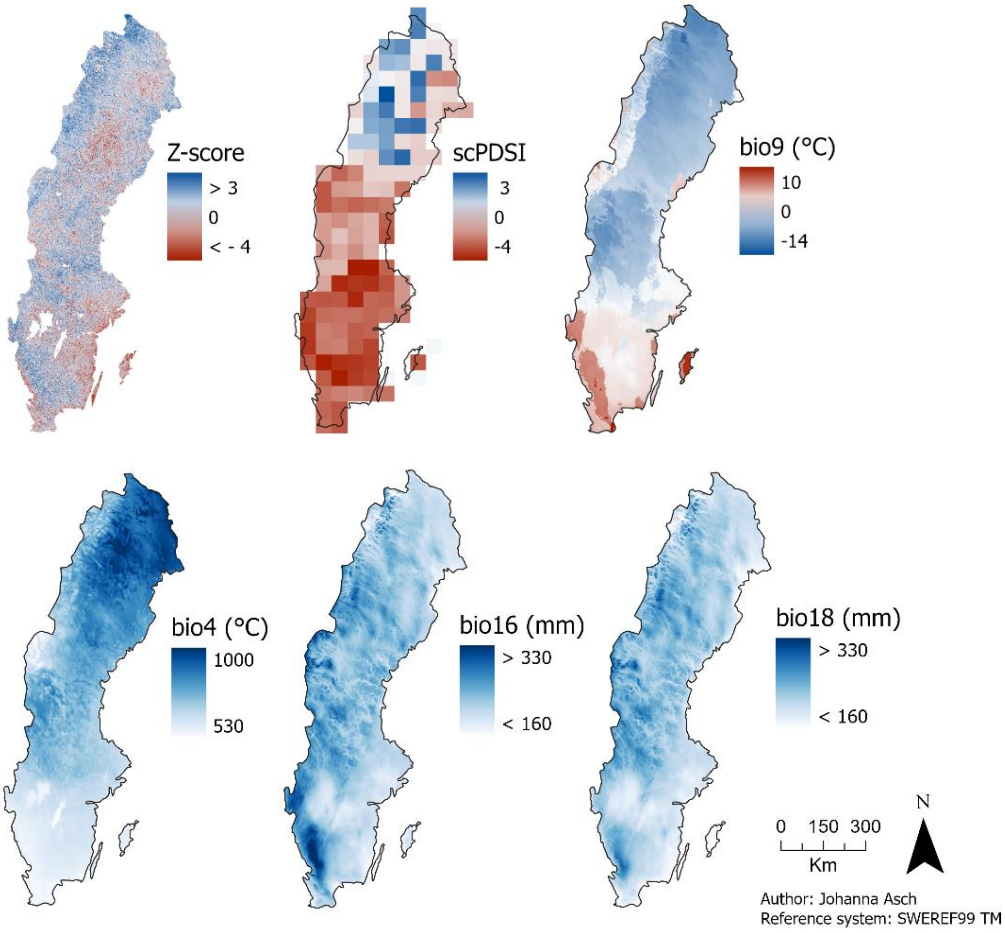

Figure 3. Spatial distribution of z-scores, scPDSI, bio9 (°C), bio4 (°C), bio16 (mm) and bio18 (mm) in Sweden. Z-scores represent Landsat EVI2 z-scores of July-September 2018. ScPDSI is a unitless drought index, negative scPDSI representing negative drought effects. Bio4-18 are bioclimatic variables, representing precipitation in the warmest (bio18) and wettest (bio16) quarter, mean temperature of the driest quarter (bio9) and temperature seasonality (bio 4). Variables are described in more detail in table 1. Spatial reference system: SWEREF99 TM.

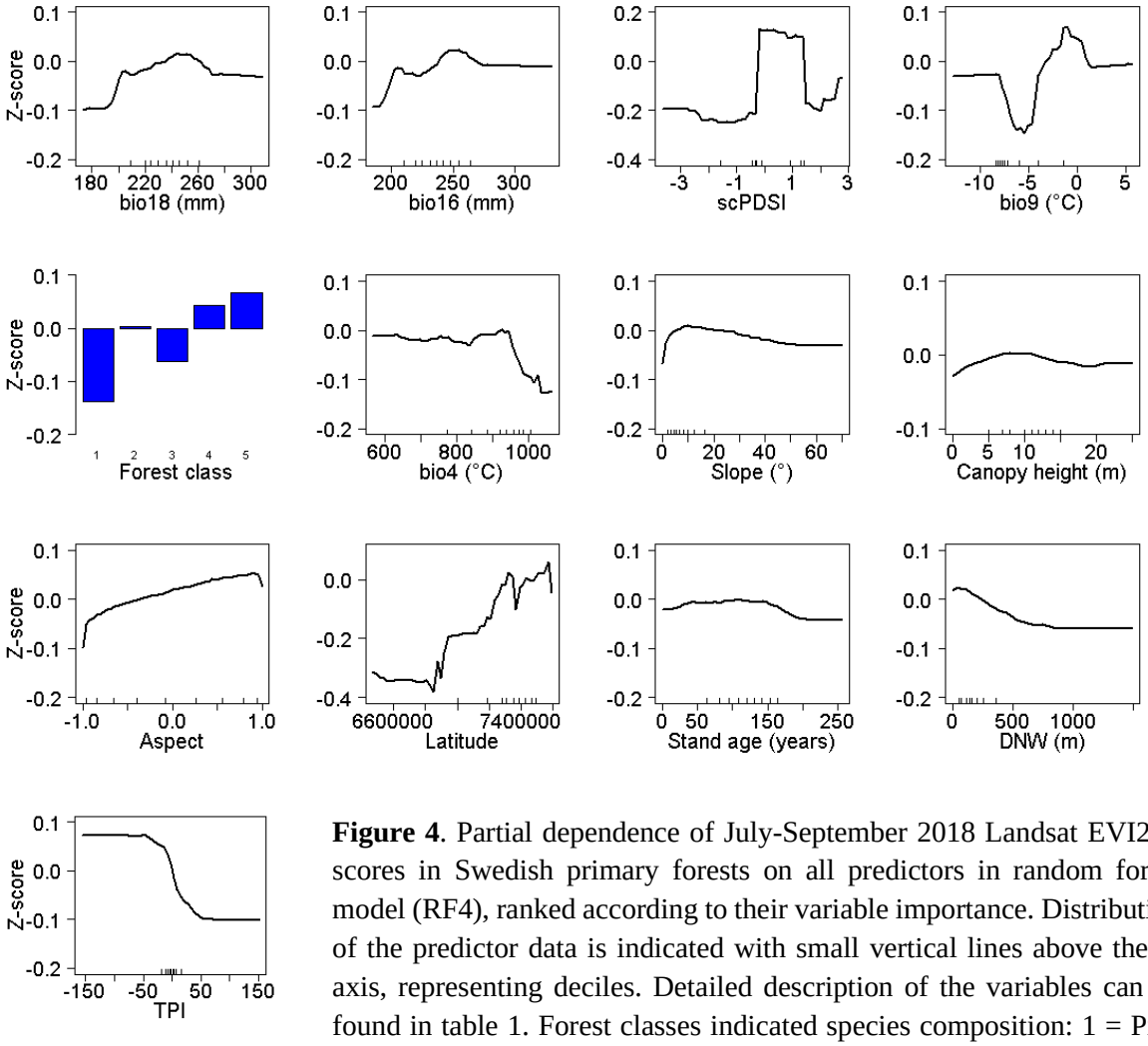

Figure 4. Partial dependence of July-September 2018 Landsat EVI2 z-scores in Swedish primary forests on all predictors in random forest model (RF4), ranked according to their variable importance. Distribution of the predictor data is indicated with small vertical lines above the x-axis, representing deciles. Detailed description of the variables can be found in table 1. Forest classes indicated species composition: 1 = Pine dominated, 2 = Spruce dominated, 3 = mixed coniferous, 4 = mixed deciduous – coniferous, 5 = deciduous. Bio4-18 are bioclimatic variables, representing precipitation in the warmest (bio18) and wettest (bio16) quarter, mean temperature of the driest quarter (bio9) and temperature seasonality (bio 4).

4.3.2 Two variable partial dependencies

Because of potential complex interaction between variables, not captured by single partial dependencies, two variable partial dependence plots were produced. The influence of latitude on topographic drought effects, is shown in figure 5. In general, z-scores were significantly lower in southern regions than in northern regions, across all aspects, slopes and TPIs (figure 5). The single partial relationship between aspect and z-scores shown in figure 4, can be observed across all latitudes (figure 5A). However, the north-south facing gradient was most pronounced in lower latitudes. Additionally, the range of z-scores shifted from ~ - 0.25 (north-facing aspects) to below -0.4 (south-facing aspects) for the southern latitudes to ~ 0.05 (north-facing aspects) to -0.05 (south-facing aspects) in high latitudes (figure 5A).

Slope effects seem to be inverted in high latitude compared to low latitudes. In low latitudes z-scores increased with increasing steepness and in high latitudes z-scores decreased with increasing steepness (figure 5B). TPI shows the most pronounced effect on z-scores compared to the other terrain indices across all latitudes. Forests located at low TPIs across the entire study area, were notably less affected by the summer 2018 drought than forests at high TPI. As it was the case for aspect. the range of z-scores shifted upwards towards z-scores > 0 with increasing latitude (figure 5C).

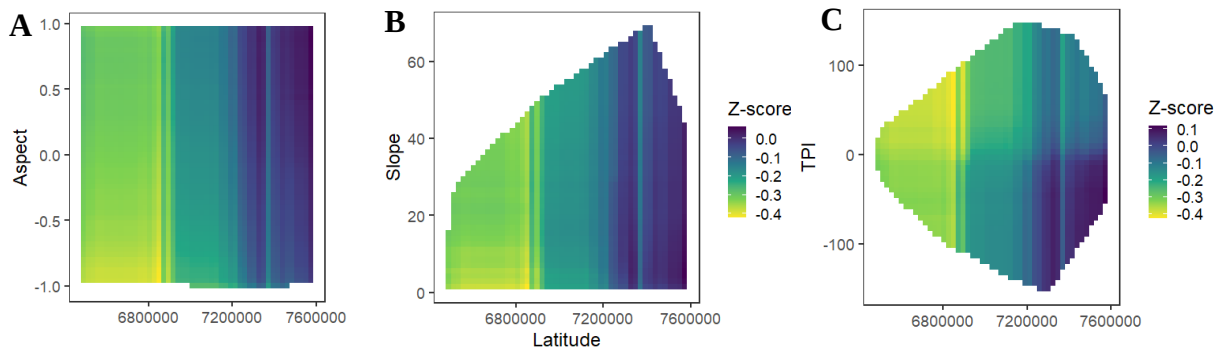

Figure 5. Two variable partial dependence of July-September 2018 Landsat EVI2 z-scores in Swedish primary forests on the topographical predictors aspect (A), slope (B) and TPI (C) in combination with latitude in random forest model RF4. TPI describes the relative elevation in a 1000 m neighbourhood. Aspect represents the north-south direction, 1.0 being north, 0.0 east and west and -1.0 south. Slope is expressed in degrees. Partial dependence was calculated with the model training data.

Partial dependencies of z-scores on TPI and aspect in combination with slope (figure 6, A and B), explain the slope effects shown in the single partial dependence plots and its relationship with latitude (figure 4 and 6B). Points on high topographic positions, and south facing aspects, likely located at flat ridges experiencing strong negative drought effects, represented by the small number of pixels with extremely low z-scores (< -0.1) in figure 6 (A and B) led to a positive relationship between z-scores and slope in the range of 0 to 10 degrees of steepness (figure 4). However, in general, for the rest of the data slope was negatively related to z-scores. North facing aspects on gentle slopes were associated with the highest z-scores > 0.5 and south facing aspects on steep slopes (> 40 degrees) showed negative z-scores < -0.1 (figure 6B).

Influences of the compass direction of the terrain were stronger on high topographic positions (TPI > 0) (figure 6C). Z-scores of forests on high topographic positions ranged from 0 (northern aspect) to - 0.15 (southern aspect) in contrast to low topographic positions (TPI < 0), where z-scores ranged from 0.1 (northern aspects) to 0.05 (southern aspects) (figure 6C). Additionally, topographic organisation of drought effects in relation to TPI was generally more pronounced on south-facing aspects than north-facing aspects (figure 6C).

The partial relationship of TPI to EVI2 z-scores was seen across all forest classes (figure 7). However, the range of z-scores was shifted significantly between classes. Deciduous forests showed z-scores between 0.15 (TPI < -50) and -0.05 (TPI > 50). In comparison pine forests had z-scores in the range of -0.1 (TPI < -50) to -0.2 (TPI > 50) (figure 7).

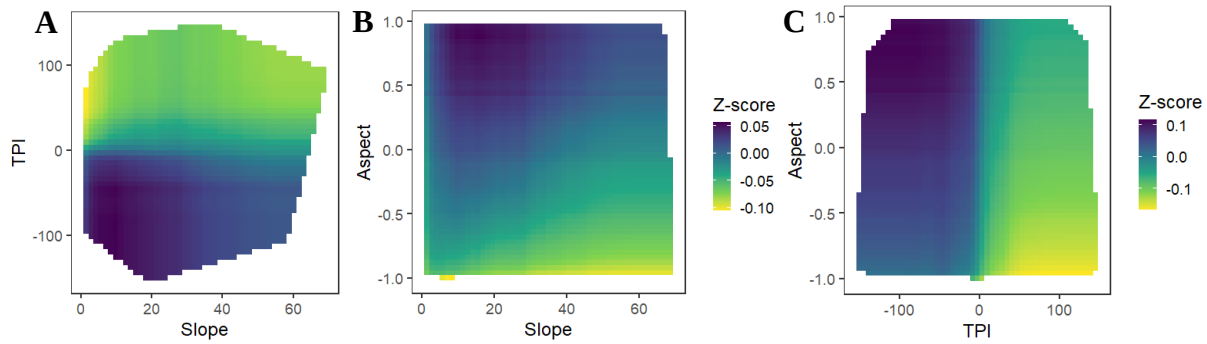

Figure 6. Two variable partial dependence of July-September 2018 Landsat EVI2 z-scores in Swedish primary forests on the predictors TPI, aspect and slope in random forest model RF4. TPI represents the relative elevation in a 1000m neighbourhood. Aspect represents the north-south direction, 1.0 being north, 0.0 east and west and -1.0 south. Slope is expressed in degrees. Partial dependence was calculated with the model training data.

The partial relationship of TPI to EVI2 z-scores was seen across all forest classes (figure 7). However, the range of z-scores was shifted significantly between classes. Deciduous forests showed z-scores between 0.15 (TPI < -50) and -0.05 (TPI > 50). In comparison pine forests had z-scores in the range of -0.1 (TPI < -50) to -0.2 (TPI > 50) (figure 7).

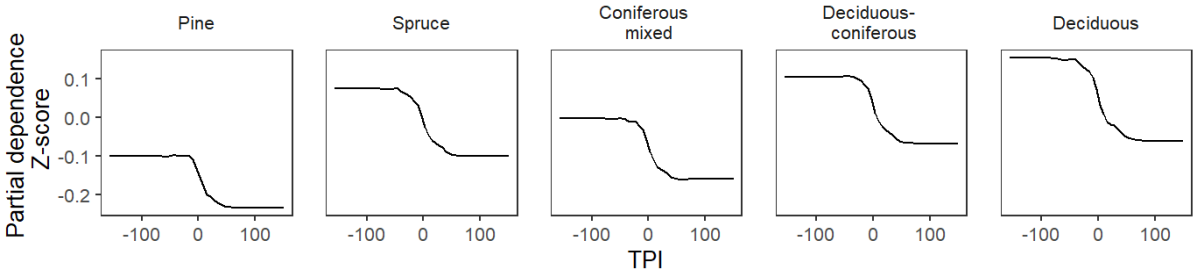

Figure 7. Two variable partial dependence of July-September 2018 Landsat EVI2 z-scores in Swedish primary forests on the predictors TPI and forest class in random forest model RF4. TPI represents the relative elevation in a 1000m neighbourhood. Partial dependence was calculated with the model training data.

5. Discussion

5.1 Predictors of drought impact

In light of projected increases in drought frequency, increasing our understanding of drought impact on forests is important for accurate predictions and assessments of future drought related risks. Local climate is modified by many interacting environmental factors including topography which influences the drought resistance of vegetation on a small spatial scale. However, especially for boreal forests knowledge regarding the influence of local topography on drought events is scarce. This knowledge gap is particularly wide for primary forests, which offer the opportunity to investigate the response of natural forest ecosystems to extreme drought events. This study aimed at contributing to filling that knowledge gap by applying a random forest modelling approach, investigating the influence of the local environment including topography and forest properties on impact of the 2018 summer drought in primary forests in Sweden.

The RFE analysis selected 13 of the predictor variables included in this analysis as the most influential on EVI2 z-scores. These predictors can be categorized as climatic predictors (bio4, bio9, bio16, bio18 and scPDSI), forest properties (forest class, stand age, canopy height, DNW), and topographical predictors (slope, aspect, TPI). The model performance exceeded expectations, capturing around 48% ($R^2 = 0.48$) of the of the variance in observed EVI2 z-scores (figure 2).

The model captured spatial patterns of drought effects well, considering the unquantified and potentially large uncertainties in explanatory variables and the satellite derived metric of drought impact as well as potentially missing variables such as soil type (figure 3 and 4). The fact that the partial dependencies show expected relationships between drought impact and the explanatory variables offer additional confidence in the model's accuracy, i.e. drier landscapes positions farther from wetlands and in areas with stronger drought (scPDSI < 0) showed more negative EVI2 z-scores than topographically wetter locations closer to wetlands experiencing less severe drought (scPDSI ≥ 0). However, the model failed to capture the extremes of the observed EVI2 z-score range, underestimating both the reduction as well as the increase in EVI2 due to drought conditions in some regions (figure 2), implying that the causes for severe negative drought impact was not captured by the explanatory variables at the resolution they were applied. Therefore, the model is likely able to capture relationships between predictors and drought effects, but underestimates drought magnitude and should only be interpreted in a qualitative way when investigating spatial z-score patterns and interaction between predictors.

By using July-September EVI this study only focused on immediate drought impact of the 2018 summer drought on forests, but forest drought responses are complex and dynamic over time and mortality reaches its maximum with a time lag after the drought event (Anderegg et al.

2019; Reinermann et al. 2019). Therefore, this study probably covers only a part of the actual drought impact from the 2018 drought experienced by forests.

In general, the results are consistent with findings of other studies in temperate and topical forest ecosystems (Goulden and Bales 2019; Schwartz et al. 2019; Kharuk et al. 2020). Partial dependence plots clearly showed the role the local topography played in creating microclimates that influenced the response of vegetation to the 2018 summer drought (figure 4 and 6). The reduction of July – September EVI2 was notably increased on divergent topographic positions such as steep slopes and ridges. Valleys bottoms and north-facing aspects strongly mitigated drought conditions, leading in some cases to a greening in less drought effected regions in the north of Sweden, due to elimination of growth limitations by temperature. As described by Dobrowski (2011), locations with these characteristics could serve as microrefugia for native species, preserving local biodiversity during the upcoming period of accelerated climate change. Contrarily to expectations the compound terrain indices TWI and HAND and the soil moisture index (SM) did not capture z-scores as effectively, or more effectively than primary terrain indices. This suggests that the exposure of a location to solar radiation and the atmospheric environment had a greater influence on direct drought effects than the relative soil moisture status.

Topographic organisation of drought impact was present in all forest classes, indicating that topographical differences in drought impact cannot solely be attributed to differences in species composition along topographic gradients. However, forest class was ranked a more important predictor of drought impact in the random forest analysis than the terrain indices were (table 3). Even though all forests experienced differences in drought effects between topographic positions, the general severity of the drought impact (the lower end of the z-score range experienced by a forest class) was determined by the forest composition (figure 7). Deciduous and spruce dominated forests were less negatively affected and even showed positive z-scores in some topographically convergent locations. In contrast pine dominated forests were generally negatively affected, regardless of the topographic position. This difference could be explained by the soils favoured by the different tree species. Pine trees are usually associated with sandy soils, which have a lower soil water retention capacity. Soil characteristics can have a significant influence on tree drought response (Rehschuh et al. 2017). Due a lack of data at sufficient resolution, however, they could not be included in this analysis. Future modelling efforts need to include data on soil types at a high resolution to clarify how the apparent effect of species composition on drought resilience, as seen in this study, is related to soil composition. Additionally, the observed EVI2 could be influenced by the understory, especially in forests with potentially less dense canopies such as pine forests. The forest classes used in this analysis only captures the dominant forest type at a certain grid cell and were reclassified to a 50 m resolution to match the resolution of the EVI2 raster. This analysis, therefore, captures general trends associated with the dominant tree type in a certain area. Differences between forests that

could influence drought impact, such as the composition of the understory, were not captured. Stand age and canopy height, were selected as important predictors during RFE, but based on the partial dependence plots no robust conclusions can be drawn about their influence on drought effects (table 3 and figure 4). Shorter and younger forests stands are believed to experience stronger negative drought effects than old forests with high canopies (Schwartz et al. 2019; Wolf 2020). However, these studies investigated differences between primary and secondary forests, where other differences in forest composition and management might have contributed to this effect.

The analysis presented here suggests that capturing the effect of local terrain on drought effects requires a sufficiently high resolution to avoid smoothing out the signal. Given the availability of satellite products, the resolution of z-scores was restricted to 50 m x 50 m in this study. This scale is likely to capture most of the local landforms, however in topographically very complex terrain some landscape variability will be lost. With other, coarser satellite products such as MODIS data topographic effects could probably not be captured at all, highlighting the importance of high-resolution data for modelling forest vegetation dynamics in the face of climate change type droughts. For future research and a detailed assessment of vulnerabilities and resilience of Swedish primary forests, maybe for the purpose of conservation, an approach with a higher spatial resolution for individual forests could allow identifying microrefugia and locations particularly vulnerable to climate change type droughts.

5.1.2 Implications for forest management

For the purpose of a clear forest ecosystem signal, without interference from human management, this study focused on primary forest ecosystems. However, since previous research found primary forests less affected by the 2018 drought than managed secondary forests the results presented here could none the less give some insight into the potential effect of management on forest drought resistance (Wolf 2020). Partial dependency of EVI2 z-scores to distance to nearest wetland, show that drought effects in primary forests were mitigated by wetlands during the 2018 drought and drought impact severity increased with increasing distance from wetlands (figure 4). This indicates that wetlands play an important role for local water resources. Extensive draining, decreasing the area of forested wetlands dramatically, could have had a significant negative impact on the drought resistance of managed forests (Hånell 1988; Jacks 2019). Additionally, our findings show that mixed stands showed combined drought effects of the individual species and therefore mitigating the negative impact on the forest as a whole. Especially mixed coniferous deciduous stands showed substantially reduced drought effect compared to coniferous forests, indicating the benefits of mixed species composition for forest drought resistance (figure 7). Most managed forests in Sweden are Norway spruce (*Picea abies*) or Scots pine (*Pinus sylvestris*) monocultures and could thus be more vulnerable to negative drought impact than primary forests. Extending this study to

include managed forests, could provide insight into differences in drought response of both forest ecosystems and aid in the effort to adapt Swedish forestry to the changing climate.

5.2 Model limitations and uncertainties

Random forests allow for a relatively high level of interpretation of the model structure, compared to other machine learning algorithms. However, there are limitations to interpreting model structure based on partial dependencies. Setting all other predictors to their average values, to reveal the influence of a single predictor on the variable in question might create combinations of conditions that are impossible in reality. Additionally, patterns in the response variable might be attributed too strongly to a certain predictor by setting other influential predictors to their average value. An example in this analysis is the partial dependency of z-scores to the topographic predictor slope. Flat or gentle slopes can experience both positive and negative z-scores depending on their TPI, since flat ridges and flat valleys experience very different exposure to drought effects. For the single partial relationship plot for slope, the occurrence of an increased number of flat ridges in southern Sweden led to a general trend of drought effects decreasing with increasing slope until 20° steepness, a pattern that is not applicable for the entire dataset (figure 4). This problem can be mitigated by combining predictors for partial dependencies, in this case slope, TPI and latitude (figure 5 and 6), but partial dependencies are limited to three dimensions or often, for the purpose of interpretability, to two dimensions.

Likely important sources of uncertainties associated with the data include the spatial and temporal resolution of the satellite data as well as the spatial resolution and quality of the DEM. The choice of Landsat EVI2 July - September composites for detecting vegetation drought impact was based on the work of Wolf (2020), who discussed the uncertainties associated with this approach in detail. In short, due to the long return time of Landsat satellites (16 days) in addition to data loss due to clouds and diminished scene quality, capturing the temporal variability of drought impact on EVI2 is difficult. The July - September composites thus offer a relatively coarse estimate of drought impact. Yet, no other satellite product offered a sufficiently high spatial resolution with an appropriately long baseline period.

All terrain indices were derived from the DEM. Uncertainties associated with the DEM such as spatial resolution and data quality are therefore propagated to the individual terrain index. The DEM used here was provided by the Swedish governmental agency Lantmäteriet and is created by aggregation of the national elevation model of 1 m resolution. Accuracy of the elevation data declines in “very hilly terrain” and with decreasing resolution of the elevation rasters created from the national elevation model (Lantmäteriet 2019). Additionally, the derivation of each individual index introduced additional uncertainty. For example, the neighbourhood on which the TPI calculation is based determines the level of detail captured by the index. Small neighbourhoods capture small hills and depressions, however loose information about more large-scale topographic patterns and vice versa (Weiss 2001). Since the best scale of the TPI

strongly depends on the size and topography of the study site, several neighbourhoods were calculated and analysed. Primary forests in Sweden differ substantially in size and complexity of the topography, therefore calculating TPI with the same neighbourhood of 1 km for all forests could lead to a loss of some of the relevant topographic signal in particularly large forests or forests with highly complex topography. Similarly, in the calculation of HAND a stream layer is created using a watershed size dependent threshold of water flow accumulation (Rennó et al. 2008). The threshold used for HAND in this study was based on the average watershed size and might not describe all forests equally well. Both indices could, thus, be underestimated in their capability to describe topographic drought effects in this study and would reveal a stronger influence in an analysis of individual forests.

5.2.1 Modelling drought impact with random forest regression

The random forest algorithm is a powerful regression tool, allowing for the analysis of large datasets with many predictors and non-linear relationships. It is relatively easy to implement, requiring the tuning of only two parameters (number of trees and number of splits) and provides the opportunity of assessing predictor importance (Breiman 2001; Grömping 2009). For data sets with many data points, such as in this study, building of the random forest can be time consuming and requires a lot of computational power. This restricted the size of the training dataset and the number of iterations of the model building process. Because of their modelling approach random forest models are subject to a certain amount of randomness in the output. In bagging, a random subset of the training data is selected for building the decision tree and at each split a set number of predictors is randomly selected from all predictors. This means, that if a predictor has a high variable importance based on the effect a permutation of the predictor would have on the model error, it is likely that this predictor is in fact important. However, due to the randomness of the algorithm it is also possible that this predictor was randomly chosen many times in the node splitting process and is therefore overestimated in its importance (Janitza et al. 2018). The recursive feature elimination approach applied here somewhat mitigates that problem, since feature importance was reassessed at each step and "unimportant" predictors will likely be ranked low in one of the steps and eliminated. Other studies have observed a tendency to overfit the training data for models built with RFE and reassessing variable importance at each run (Svetnik et al. 2004). Model accuracy in the model validation, however, did not decrease significantly from the second model (RF2) to the last (RF4), suggesting that this might not be an issue in this approach (table 3). The four steps of feature elimination as applied here might not be enough to avoid the overestimation of a predictor completely. Variable selection with random forests is still a subject of ongoing research. Several approaches exist for a more robust variable selection; but their success depends on the nature of the data and the research aim. Most approaches were not applicable in this study, either because of limited computational power or because of the data types they were designed for (Szymczak et al. 2016; Greenwell et al. 2018; Janitza et al. 2018). In general, more robust results could potentially be achieved by increasing the number of iterations, such as in the

variable selection method r2VIM proposed by Szymczak et al. (2016). Since important features will have relatively high variable importance scores in most runs, variables can be ranked according to their relative importance in all runs.

Another factor potentially influencing variable importance is between predictor correlation (Strobl et al. 2007). Many predictors used in this study are naturally highly correlated, such as bioclimatic variables and latitude or TWI and HAND. RF-CART in combination with permutation variable importance is the most widely applied RF model. It has been shown to be biased in the presence of within predictor correlation (Strobl et al. 2007; Zhang and Yang 2020). Many approaches have been suggested to circumvent this problem, showing that the best choice of RF and variable importance measure is very aim and data dependent (Zhang and Yang 2020). Conditional Permutation Variable Importance Measure (CPVIM) based on a different type of decision tree, the Conditional Inference Tree (CIT) have been suggested to avoid problems with correlated predictors, showing more consistent results (Hothorn et al. 2006; Strobl et al. 2008). CIT random forests require more computational power and have not always shown more accurate results than RF-CART (Zhang and Yang 2020). For this study, because of the required memory space and time to build a RF-CIT model, it was not possible to compare RF approaches and the variable importance measure CPVIM with the applied permutation variable importance. For further research on this topic, comparing variable importance rankings of both approaches could contribute to a more accurate model of drought impact predictors.

6. Conclusion

This study found that topography was a relevant modulator of direct drought effects in primary forests during the summer drought in 2018. Topographic landforms both exposed vegetation to severe drought conditions (ridges, south-facing aspects) and created microrefugia (valleys, north facing aspects), protecting vegetation from drought. Surprisingly, topographic organisation of drought effects was best described by the primary terrain indices aspect, slope, and TPI and not as may be expected by the more complex compound terrain indices such as TWI. Drought impact and the local environment showed clear interactions, despite the considerable uncertainties associated with remotely sensed vegetation indices and DEM derived terrain indices. This highlights the need for studying vegetation dynamics at resolutions that differentiate between topographically wet and dry locations. Especially for accurate assessments of future climate-change related risks for forest ecosystems, the incorporation of topography would improve model predictions.

Given the previous findings that primary forests were generally affected less than managed forests this project suggests that the establishment of monocultures on drained soils may contribute to the increased drought vulnerability of managed secondary forests.

7. References

Adams, H. R., H. R. Barnard, and A. K. Loomis. 2014. Topography alters tree growth–climate relationships in a semi-arid forested catchment. *Ecosphere* 5: art148. doi:https://doi.org/10.1890/ES14-00296.1.

Afshari, S., A. A. Tavakoly, M. A. Rajib, X. Zheng, M. L. Follum, E. Omranian, and B. M. Fekete. 2018. Comparison of new generation low-complexity flood inundation mapping tools with a hydrodynamic model. *Journal of Hydrology* 556: 539–556. doi:https://doi.org/10.1016/j.jhydrol.2017.11.036.

Ågren, A. M., W. Lidberg, M. Strömgren, J. Ogilvie, and P. A. Arp. 2014. Evaluating digital terrain indices for soil wetness mapping-a Swedish case study. *Hydrology and Earth System Sciences* 18: 3623–3634. doi:10.5194/hess-18-3623-2014.

Ahlström, A., G. E. De Jong, W. Nijland, and T. Tagesson. 2020. Primary productivity of managed and pristine forests in Sweden. *Environmental Research Letters* 15. doi:10.1088/1748-9326/ab9a6b.

Allen, C. D., A. K. Macalady, H. Chenchouni, D. Bachelet, N. McDowell, M. Vennetier, T. Kitzberger, A. Rigling, et al. 2010. A global overview of drought and heat-induced tree mortality reveals emerging climate change risks for forests. *Forest Ecology and Management* 259: 660–684. doi:10.1016/j.foreco.2009.09.001.

Allen, C. D., D. D. Breshears, and N. G. McDowell. 2015. On underestimation of global vulnerability to tree mortality and forest die-off from hotter drought in the Anthropocene. *Ecosphere* 6: art129. doi:https://doi.org/10.1890/ES15-00203.1.

Anderegg, W. R. L., A. Flint, C. Y. Huang, L. Flint, J. A. Berry, F. W. Davis, J. S. Sperry, and C. B. Field. 2015. Tree mortality predicted from drought-induced vascular damage. *Nature Geoscience* 8: 367–371. doi:10.1038/ngeo2400.

Anderegg, W. R. L., L. D. L. Anderegg, and C. Huang. 2019. Testing early warning metrics for drought-induced tree physiological stress and mortality. *Global Change Biology* 25: 2459–2469. doi:https://doi.org/10.1111/gcb.14655.

Barichivich, J., T. J. Osborn, I. Harris, G. van der Schrier, and P. D. Jones. 2018. Drought [in "State of the Climate in 2018"]. *Bulletin of the American Meteorological Society* 100: 1–306.

Bastos, A., P. Ciais, P. Friedlingstein, S. Sitch, J. Pongratz, L. Fan, J. P. Wigneron, U. Weber, et al. 2020. Direct and seasonal legacy effects of the 2018 heat wave and drought on European ecosystem productivity. *Science Advances* 6: 1–14. doi:10.1126/sciadv.aba2724.

Beven, K. J., and M. J. Kirkby. 1979. A physically based, variable contributing area model of basin hydrology / Un modèle à base physique de zone d'appel variable de l'hydrologie du bassin versant. *Hydrological Sciences Bulletin* 24. Taylor & Francis: 43–69. doi:10.1080/02626667909491834.

Bonan, G. B. 2008. Forests and climate change: Forcings, feedbacks, and the climate benefits of forests. *Science* 320: 1444–1449. doi:10.1126/science.1155121.

Breiman, L. 2001. Random Forests. *Machine Learning* 45: 5–32. doi:10.1023/A:1010933404324.

Breshears, D. D., N. S. Cobb, P. M. Rich, K. P. Price, C. D. Allen, R. G. Balice, W. H. Romme, J. H. Kastens, et al. 2005. Regional vegetation die-off in response to global-change-type drought. *Proceedings of the National Academy of Sciences* 102. National Academy of Sciences: 15144–15148. doi:10.1073/pnas.0505734102.

Buchanan, B. P., M. Fleming, R. L. Schneider, B. K. Richards, J. Archibald, Z. Qiu, and M. T. Walter. 2014. Evaluating topographic wetness indices across central New York agricultural landscapes. *Hydrology and Earth System Sciences* 18: 3279–3299. doi:10.5194/hess-18-3279-2014.

Buchwald, E. 2005. *A hierarchical terminology for more or less natural forests in relation to sustainable management and biodiversity conservation*. Rome.
Buras, A., A. Rammig, and C. S. Zang. 2020. Quantifying impacts of the 2018 drought on European ecosystems in comparison to 2003. *Biogeosciences* 17: 1655–1672. doi:10.5194/bg-17-1655-2020.
Cartwright, J. M., C. E. Littlefield, J. L. Michalak, J. J. Lawler, and S. Z. Dobrowski. 2020. Topographic, soil, and climate drivers of drought sensitivity in forests and shrublands of the Pacific Northwest, USA. *Scientific Reports* 10. Nature Publishing Group UK: 1–13. doi:10.1038/s41598-020-75273-5.
Chuvieco, E. 2016. *Fundamentals of Satellite Remote Sensing - An environmental approach*. Boca Raton: CRC Press.
Ciais, P., M. Reichstein, N. Viovy, A. Granier, J. Ogée, V. Allard, M. Aubinet, N. Buchmann, et al. 2005. Europe-wide reduction in primary productivity caused by the heat and drought in 2003. *Nature* 437: 529–533. doi:10.1038/nature03972.
Copernicus Climate Change Service. 2018. *European State of the Climate 2018, Full report: climate.copernicus.eu/ESOTC/2018*.
Díaz-Uriarte, R., and S. Alvarez de Andrés. 2006. Gene selection and classification of microarray data using random forest. *BMC Bioinformatics* 7: 3. doi:10.1186/1471-2105-7-3.
Dilts, T. E. 2015. Topography Tools for ArcGIS 10.1. University of Nevada Reno.
Dobrowski, S. Z. 2011. A climatic basis for microrefugia: the influence of terrain on climate. *Global Change Biology* 17: 1022–1035. doi:https://doi.org/10.1111/j.1365-2486.2010.02263.x.
Esteban, E. J. L., C. V Castilho, K. L. Melgaço, and F. R. C. Costa. 2021. The other side of droughts: wet extremes and topography as buffers of negative drought effects in an Amazonian forest. *New Phytologist* 229: 1995–2006. doi:https://doi.org/10.1111/nph.17005.
FAO. 2010. *Global Forest Resource Assessment 2010: Terms and Definitions*. Rome; Italy.
Fekedulegn, D., R. R. Hicks, and J. J. Colbert. 2003. Influence of topographic aspect, precipitation and drought on radial growth of four major tree species in an Appalachian watershed. *Forest Ecology and Management* 177: 409–425. doi:10.1016/S0378-1127(02)00446-2.
Fick, S. E., and R. J. Hijmans. 2017. WorldClim 2: new 1-km spatial resolution climate surfaces for global land areas. *International Journal of Climatology* 37: 4302–4315. doi:https://doi.org/10.1002/joc.5086.
Fridley, J. D. 2009. Downscaling Climate over Complex Terrain: High Finescale (<1000 m) Spatial Variation of Near-Ground Temperatures in a Montane Forested Landscape (Great Smoky Mountains). *Journal of Applied Meteorology and Climatology* 48. Boston MA, USA: American Meteorological Society: 1033–1049. doi:10.1175/2008JAMC2084.1.
Fu, Z., P. Ciais, A. Bastos, P. C. Stoy, H. Yang, J. K. Green, B. Wang, K. Yu, et al. 2020. Sensitivity of gross primary productivity to climatic drivers during the summer drought of 2018 in Europe. *Philosophical Transactions of the Royal Society B: Biological Sciences* 375: 20190747. doi:10.1098/rstb.2019.0747.
Gauthier, S., P. Bernier, T. Kuuluvainen, A. Z. Shvidenko, and D. G. Schepaschenko. 2015. Boreal forest health and global change. *Science* 349: 819–822. doi:10.1126/science.aaa9092.
Goulden, M. L., and R. C. Bales. 2019. California forest die-off linked to multi-year deep soil drying in 2012–2015 drought. *Nature Geoscience* 12. Springer US: 632–637. doi:10.1038/s41561-019-0388-5.
Greenwell, B. M. 2017. pdp: An R Package for Constructing Partial Dependence Plots. *The R Journal* 9: 421–436.

Greenwell, B. M., B. C. Boehmke, and A. J. McCarthy. 2018. A Simple and Effective Model-Based Variable Importance Measure.

Grömping, U. 2009. Variable Importance Assessment in Regression: Linear Regression versus Random Forest. *The American Statistician* 63. Taylor & Francis: 308–319. doi:10.1198/tast.2009.08199.

Hanel, M., O. Rakovec, Y. Markonis, P. Máca, L. Samaniego, J. Kyselý, and R. Kumar. 2018. Revisiting the recent European droughts from a long-term perspective. *Scientific Reports* 8: 9499. doi:10.1038/s41598-018-27464-4.

Hånell, B. 1988. Postdrainage forest productivity of peatlands in Sweden. *Canadian Journal of Forest Research* 18: 1443–1456. doi:10.1139/x88-223.

Hari, V., O. Rakovec, Y. Markonis, M. Hanel, and R. Kumar. 2020. Increased future occurrences of the exceptional 2018-2019 Central European drought under global warming. *Scientific reports* 10. Nature Publishing Group UK: 12207. doi:10.1038/s41598-020-68872-9.

Hawthorne, S., and C. F. Miniat. 2018. Topography may mitigate drought effects on vegetation along a hillslope gradient. *Ecohydrology* 11. doi:10.1002/eco.1825.

Hothorn, T., K. Hornik, and A. Zeileis. 2006. Unbiased Recursive Partitioning: A Conditional Inference Framework. *Journal of Computational and Graphical Statistics* 15. Taylor & Francis: 651–674. doi:10.1198/106186006X133933.

Hoylman, Z. H., K. G. Jencso, J. Hu, J. T. Martin, Z. A. Holden, C. A. Seielstad, and E. M. Rowell. 2018. Hillslope Topography Mediates Spatial Patterns of Ecosystem Sensitivity to Climate. *Journal of Geophysical Research: Biogeosciences* 123: 353–371. doi:https://doi.org/10.1002/2017JG004108.

Hoylman, Z. H., K. G. Jencso, J. Hu, Z. A. Holden, B. Allred, S. Dobrowski, N. Robinson, J. T. Martin, et al. 2019. The Topographic Signature of Ecosystem Climate Sensitivity in the Western United States. *Geophysical Research Letters* 46: 14508–14520. doi:https://doi.org/10.1029/2019GL085546.

Huang, C. Y., and W. R. L. Anderegg. 2012. Large drought-induced aboveground live biomass losses in southern Rocky Mountain aspen forests. *Global Change Biology* 18: 1016–1027. doi:10.1111/j.1365-2486.2011.02592.x.

Huete, A., K. Didan, T. Miura, E. P. Rodriguez, X. Gao, and L. G. Ferreira. 2002. Overview of the radiometric and biophysical performance of the MODIS vegetation indices. *Remote Sensing of Environment* 83: 195–213. doi:https://doi.org/10.1016/S0034-4257(02)00096-2.

IPCC. 2014. *Climate Change 2014: Synthesis Report. Contribution of Working Groups I, II and III to the Fifth Assessment Report of the Intergovernmental Panel on Climate Change [Core Writing Team, R.K. Pachauri and L.A. Meyer (eds.)]*. Geneva; Switzerland.

Jacks, G. 2019. Drainage in Sweden -the past and new developments. *Acta Agriculturae Scandinavica, Section B — Soil \& Plant Science* 69. Taylor & Francis: 405–410. doi:10.1080/09064710.2019.1586991.

Janitza, S., E. Celik, and A.-L. Boulesteix. 2018. A computationally fast variable importance test for random forests for high-dimensional data. *Advances in Data Analysis and Classification* 12: 885–915. doi:10.1007/s11634-016-0276-4.

Jenness, J. 2006. *Topographic Position Index (TPI) v. 1.2*. *Topographic Position Index (TPI) extension for ArcView 3.x, v. 1.2*.

Jiang, Z., A. R. Huete, K. Didan, and T. Miura. 2008. Development of a two-band enhanced vegetation index without a blue band. *Remote Sensing of Environment* 112: 3833–3845. doi:https://doi.org/10.1016/j.rse.2008.06.006.

Johnson, J. M., D. Munasinghe, D. Eyelade, and S. Cohen. 2019. An integrated evaluation of the National Water Model (NWM)--Height Above Nearest Drainage (HAND) flood

mapping methodology. *Natural Hazards and Earth System Sciences* 19: 2405–2420. doi:10.5194/nhess-19-2405-2019.
Jönsson, A. M., F. Lagergren, and B. Smith. 2015. Forest management facing climate change - an ecosystem model analysis of adaptation strategies. *Mitigation and Adaptation Strategies for Global Change* 20: 201–220. doi:10.1007/s11027-013-9487-6.
Kharuk, V. I., S. T. Im, I. A. Petrov, M. L. Dvinskaya, A. S. Shushpanov, and A. S. Golyukov. 2020. Climate-driven conifer mortality in Siberia. *Global Ecology and Biogeography*: 543–556. doi:10.1111/geb.13243.
Kimball, S., M. E. Lulow, K. R. Balazs, and T. E. Huxman. 2017. Predicting drought tolerance from slope aspect preference in restored plant communities. *Ecology and Evolution* 7: 3123–3131. doi:https://doi.org/10.1002/ece3.2881.
Kopecký, M., and Š. Čížková. 2010. Using topographic wetness index in vegetation ecology: does the algorithm matter? *Applied Vegetation Science* 13: 450–459. doi:https://doi.org/10.1111/j.1654-109X.2010.01083.x.
Kramer, P. J. 1963. Water Stress and Plant Growth. *Agronomy Journal* 55: 31–35. doi:https://doi.org/10.2134/agronj1963.00021962005500010013x.
Kramm, T., D. Hoffmeister, C. Curdt, S. Maleki, F. Khormali, and M. Kehl. 2017. Accuracy Assessment of Landform Classification Approaches on Different Spatial Scales for the Iranian Loess Plateau. *ISPRS International Journal of Geo-Information* 6. doi:10.3390/ijgi6110366.
Lantmäteriet. 2019. *Quality description of National Elevation Model*.
Lantmäteriet. 2021. GSD-Elevation data, grid 50 +. https://maps.slu.se. Accessed February 10.
Letts, M. G., K. N. Nakonechny, K. E. Van Gaalen, and C. M. Smith. 2009. Physiological acclimation of Pinus flexilis to drought stress on contrasting slope aspects in Waterton Lakes National Park, Alberta, Canada. *Canadian Journal of Forest Research* 39: 629–641. doi:10.1139/X08-206.
Liaw, A., and M. Wiener. 2002. Classification and Regression by randomForest. *R News* 2: 18–22.
Lindroth, A., J. Holst, M. L. Linderson, M. Aurela, T. Biermann, M. Heliasz, J. Chi, A. Ibrom, et al. 2021. Erratum: Effects of drought and meteorological forcing on carbon and water fluxes in Nordic forests during the dry summer of 2018 (Philosophical Transactions of the Royal Society B: Biological Sciences (2020) 375 (20190516) DOI: 10.1098/rstb.2019.0516). *Philosophical Transactions of the Royal Society B: Biological Sciences* 376. doi:10.1098/rstb.2020.0453.
Luyssaert, S., E.-D. Schulze, A. Börner, A. Knohl, D. Hessenmöller, B. E. Law, P. Ciais, and J. Grace. 2008. Old-growth forests as global carbon sinks. *Nature* 455: 213–215. doi:10.1038/nature07276.
Ma, Z., C. Peng, Q. Zhu, H. Chen, G. Yu, W. Li, X. Zhou, W. Wang, et al. 2012. Regional drought-induced reduction in the biomass carbon sink of Canada's boreal forests. *Proceedings of the National Academy of Sciences of the United States of America* 109: 2423–2427. doi:10.1073/pnas.1111576109.
McDowell, N., W. T. Pockman, C. D. Allen, D. D. Breshears, N. Cobb, T. Kolb, J. Plaut, J. Sperry, et al. 2008. Mechanisms of plant survival and mortality during drought: why do some plants survive while others succumb to drought? *New Phytologist* 178: 719–739. doi:https://doi.org/10.1111/j.1469-8137.2008.02436.x.
Miller, P. C., and D. K. Poole. 1983. The influence of annual precipitation, topography, and vegetative cover on soil moisture and summer drought in southern California. *Oecologia* 56: 385–391. doi:10.1007/BF00379717.
Mishra, A. K., and V. P. Singh. 2010. A review of drought concepts. *Journal of Hydrology* 391: 202–216. doi:https://doi.org/10.1016/j.jhydrol.2010.07.012.

Muukkonen, P., S. Nevalainen, M. Lindgren, and M. Peltoniemi. 2015. Spatial occurrence of drought-associated damages in Finnish boreal forests: Results from forest condition monitoring and GIS analysis. *Boreal Environment Research* 20: 172–180.
Naturvårdsverket. 2019a. Markfuktighetsindex [soil moisture index].
Naturvårdsverket. 2019b. Nationella marktäckedata 2018 basskikt [National land cover map 2018 base layer].
Naturvårdsverket. 2021. *Metrias markfuktighetsindex [Metria's soil moisture index]*.
Nobre, A. D., L. A. Cuartas, M. Hodnett, C. D. Rennó, G. Rodrigues, A. Silveira, M. Waterloo, and S. Saleska. 2011. Height Above the Nearest Drainage - a hydrologically relevant new terrain model. *Journal of Hydrology* 404: 13–29. doi:10.1016/j.jhydrol.2011.03.051.
Noce, S., L. Caporaso, and M. Santini. 2020. A new global dataset of bioclimatic indicators. *Scientific Data* 7: 398. doi:10.1038/s41597-020-00726-5.
Pan, Y., R. A. Birdsey, J. Fang, R. Houghton, P. E. Kauppi, W. A. Kurz, O. L. Phillips, A. Shvidenko, et al. 2011. A Large and Persistent Carbon Sink in the World{\textquoteright}s Forests. *Science* 333. American Association for the Advancement of Science: 988–993. doi:10.1126/science.1201609.
Park, H., K. Kim, and D. kun Lee. 2019. Prediction of Severe Drought Area Based on Random Forest: Using Satellite Image and Topography Data. *Water* 11. doi:10.3390/w11040705.
Pasho, E., J. J. Camarero, M. de Luis, and S. M. Vicente-Serrano. 2012. Factors driving growth responses to drought in Mediterranean forests. *European Journal of Forest Research* 131: 1797–1807. doi:10.1007/s10342-012-0633-6.
Pullanagari, R. R., G. Kereszturi, and I. Yule. 2018. Integrating Airborne Hyperspectral, Topographic, and Soil Data for Estimating Pasture Quality Using Recursive Feature Elimination with Random Forest Regression. *Remote Sensing* 10. doi:10.3390/rs10071117.
Raduła, M. W., T. H. Szymura, and M. Szymura. 2018. Topographic wetness index explains soil moisture better than bioindication with Ellenberg's indicator values. *Ecological Indicators* 85: 172–179. doi:https://doi.org/10.1016/j.ecolind.2017.10.011.
Rahman, A. F., D. A. Sims, V. D. Cordova, and B. Z. El-Masri. 2005. Potential of MODIS EVI and surface temperature for directly estimating per-pixel ecosystem C fluxes. *Geophysical Research Letters* 32. doi:https://doi.org/10.1029/2005GL024127.
Rehschuh, R., T. Mette, A. Menzel, and A. Buras. 2017. Soil properties affect the drought susceptibility of Norway spruce. *Dendrochronologia* 45: 81–89. doi:https://doi.org/10.1016/j.dendro.2017.07.003.
Reinermann, S., U. Gessner, S. Asam, C. Kuenzer, and S. Dech. 2019. The Effect of Droughts on Vegetation Condition in Germany: An Analysis Based on Two Decades of Satellite Earth Observation Time Series and Crop Yield Statistics. *Remote Sensing* 11. doi:10.3390/rs11151783.
Rennó, C. D., A. D. Nobre, L. A. Cuartas, J. V. Soares, M. G. Hodnett, J. Tomasella, and M. J. Waterloo. 2008. HAND, a new terrain descriptor using SRTM-DEM: Mapping terra-firme rainforest environments in Amazonia. *Remote Sensing of Environment* 112: 3469–3481. doi:https://doi.org/10.1016/j.rse.2008.03.018.
De Reu, J., J. Bourgeois, M. Bats, A. Zwertvaegher, V. Gelorini, P. De Smedt, W. Chu, M. Antrop, et al. 2013. Application of the topographic position index to heterogeneous landscapes. *Geomorphology* 186. Elsevier B.V.: 39–49. doi:10.1016/j.geomorph.2012.12.015.
Sabatini, F. M., S. Burrascano, W. S. Keeton, C. Levers, M. Lindner, F. Pötzschner, P. J. Verkerk, J. Bauhus, et al. 2018. Where are Europe's last primary forests? *Diversity and Distributions* 24: 1426–1439. doi:10.1111/ddi.12778.

Samaniego, L., S. Thober, R. Kumar, N. Wanders, O. Rakovec, M. Pan, M. Zink, J. Sheffield, et al. 2018. Anthropogenic warming exacerbates European soil moisture droughts. *Nature Climate Change* 8: 421–426. doi:10.1038/s41558-018-0138-5.

Schietti, J., T. Emilio, C. D. Rennó, D. P. Drucker, F. R. C. Costa, A. Nogueira, F. B. Baccaro, F. Figueiredo, et al. 2014. Vertical distance from drainage drives floristic composition changes in an Amazonian rainforest. *Plant Ecology \& Diversity* 7. Taylor & Francis: 241–253. doi:10.1080/17550874.2013.783642.

Schmidt, F., and A. Persson. 2003. Comparison of DEM Data Capture and Topographic Wetness Indices. *Precision Agriculture* 4: 179–192. doi:10.1023/A:1024509322709.

van der Schrier, G., J. Barichivich, K. R. Briffa, and P. D. Jones. 2013. A scPDSI-based global data set of dry and wet spells for 1901–2009. *Journal of Geophysical Research: Atmospheres* 118: 4025–4048. doi:https://doi.org/10.1002/jgrd.50355.

Schubert, P., F. Lagergren, M. Aurela, T. Christensen, A. Grelle, M. Heliasz, L. Klemedtsson, A. Lindroth, et al. 2012. Modeling GPP in the Nordic forest landscape with MODIS time series data—Comparison with the MODIS GPP product. *Remote Sensing of Environment* 126: 136–147. doi:https://doi.org/10.1016/j.rse.2012.08.005.

Schwartz, N. B., A. M. Budsock, and M. Uriarte. 2019. Fragmentation, forest structure, and topography modulate impacts of drought in a tropical forest landscape. *Ecology* 100. doi:10.1002/ecy.2677.

Schwartz, N. B., X. Feng, R. Muscarella, N. G. Swenson, M. N. Umaña, J. K. Zimmerman, and M. Uriarte. 2020. Topography and Traits Modulate Tree Performance and Drought Response in a Tropical Forest. *Frontiers in Forests and Global Change* 3: 1–14. doi:10.3389/ffgc.2020.596256.

Seidl, R., D. Thom, M. Kautz, D. Martin-Benito, M. Peltoniemi, G. Vacchiano, J. Wild, D. Ascoli, et al. 2017. Forest disturbances under climate change Europe PMC Funders Group. *Nat Clim Change* 7: 395–402. doi:10.1038/nclimate3303.Forest.

Senf, C., D. Pflugmacher, Y. Zhiqiang, J. Sebald, J. Knorn, M. Neumann, P. Hostert, and R. Seidl. 2018. Canopy mortality has doubled in Europe's temperate forests over the last three decades. *Nature Communications* 9: 1–8. doi:10.1038/s41467-018-07539-6.

Sims, D. A., A. F. Rahman, V. D. Cordova, B. Z. El-Masri, D. D. Baldocchi, L. B. Flanagan, A. H. Goldstein, D. Y. Hollinger, et al. 2006. On the use of MODIS EVI to assess gross primary productivity of North American ecosystems. *Journal of Geophysical Research: Biogeosciences* 111. doi:https://doi.org/10.1029/2006JG000162.

SLU. 2010. *kNN-Sverige - Aktuella kartdata över skogsmarken, årgång 2005 och 2010*.

SMHI. 2018. Somaren 2018 - Extremt varm og solig (Summer 2018 - extremely warm and sunny).

Strobl, C., A.-L. Boulesteix, A. Zeileis, and T. Hothorn. 2007. Bias in random forest variable importance measures: Illustrations, sources and a solution. *BMC Bioinformatics* 8: 25. doi:10.1186/1471-2105-8-25.

Strobl, C., A.-L. Boulesteix, T. Kneib, T. Augustin, and A. Zeileis. 2008. Conditional variable importance for random forests. *BMC Bioinformatics* 9: 307. doi:10.1186/1471-2105-9-307.

Svetnik, V., A. Liaw, C. Tong, and T. Wang. 2004. Application of Breiman's Random Forest to Modeling Structure-Activity Relationships of Pharmaceutical Molecules. In *Multiple Classifier Systems*, ed. F. Roli, J. Kittler, and T. Windeatt, 334–343. Berlin, Heidelberg: Springer Berlin Heidelberg.

Swetnam, T. L., P. D. Brooks, H. R. Barnard, A. A. Harpold, and E. L. Gallo. 2017. Topographically driven differences in energy and water constrain climatic control on forest carbon sequestration. *Ecosphere* 8: e01797. doi:https://doi.org/10.1002/ecs2.1797.

Szymczak, S., E. Holzinger, A. Dasgupta, J. D. Malley, A. M. Molloy, J. L. Mills, L. C. Brody, D. Stambolian, et al. 2016. r2VIM: A new variable selection method for random

forests in genome-wide association studies. *BioData Mining* 9: 7. doi:10.1186/s13040-016-0087-3.

Thompson, R. L., G. Broquet, C. Gerbig, T. Koch, M. Lang, G. Monteil, S. Munassar, A. Nickless, et al. 2020. Changes in net ecosystem exchange over Europe during the 2018 drought based on atmospheric observations. *Philosophical Transactions of the Royal Society B: Biological Sciences* 375: 20190512. doi:10.1098/rstb.2019.0512.

Thornthwaite, C. W. 1953. A charter for climatology. *Meteorological Organization Bulletin* 2.

Vidal-Macua, J. J., M. Ninyerola, A. Zabala, C. Domingo-Marimon, and X. Pons. 2017. Factors affecting forest dynamics in the Iberian Peninsula from 1987 to 2012. The role of topography and drought. *Forest Ecology and Management* 406: 290–306. doi:10.1016/j.foreco.2017.10.011.

Weiss, a. 2001. Topographic position and landforms analysis. *Poster presentation, ESRI User Conference, San Diego, CA* 64: 227–245.

Wells, N., S. Goddard, and M. J. Hayes. 2004. A Self-Calibrating Palmer Drought Severity Index. *Journal of Climate* 17. Boston MA, USA: American Meteorological Society: 2335–2351. doi:10.1175/1520-0442(2004)017<2335:ASPDSI>2.0.CO;2.

Wilhite, D. A., and M. H. Glantz. 1985. Understanding: the Drought Phenomenon: The Role of Definitions. *Water International* 10. Routledge: 111–120. doi:10.1080/02508068508686328.

Wilson, J. P. 2012. Digital terrain modeling. *Geomorphology* 137: 107–121. doi:https://doi.org/10.1016/j.geomorph.2011.03.012.

Wolf, J. 2020. A remote-sensing approach to studying drought resistance in Swedish old-growth and production forests. Student Thesis Series INES.

Zhang, F., and X. Yang. 2020. Improving land cover classification in an urbanized coastal area by random forests: The role of variable selection. *Remote Sensing of Environment* 251: 112105. doi:https://doi.org/10.1016/j.rse.2020.112105.

Zheng, X., D. G. Tarboton, D. R. Maidment, Y. Y. Liu, and P. Passalacqua. 2018. River Channel Geometry and Rating Curve Estimation Using Height above the Nearest Drainage. *JAWRA Journal of the American Water Resources Association* 54: 785–806. doi:https://doi.org/10.1111/1752-1688.12661.